

Reviewed Preprint

v1 • April 10, 2026

Not revised

✉ For correspondence:

lyonam@purdue.edu

* Authors contributed equally to the work.

Author contributions: I.J.F., K.S., N.A.L., and A.M.L. designed studies; K.S., I.J.F., W.J., K.O., K.M., E.G.K., M.V.C., T.K. and N.A.L. performed experiments; I.J.F., K.S., N.A.L. and A.M.L. analyzed and interpreted data; A.I. and E.K. provided key reagents; I.J.F., N.A.L., and A.M.L. wrote the manuscript.

Competing interests: No competing interests declared

Funding: See [page 28](#)

Reviewing editor: John Janetzko, University of Colorado Anschutz Medical Campus, United States

© 2026, Fisher et al. This article is distributed under the terms of the

[Creative Commons Attribution](#)

[License](#), which permits unrestricted use and redistribution provided that the original author and source are credited.

Gβγ engages PLCβ3 at multiple sites to reorient and facilitate its activation

Isaac J Fisher^{1,*}, Kanishka Senarath^{2,*}, Kennedy Outlaw¹, Kaushik Muralidharan^{3,4}, Elisabeth E Garland-Kuntz¹,

Michelle Van Camp¹, Tommy Komay¹, Asuka Inoue^{5,6}, Eva Kostenis⁷, Nevin A Lambert², Angeline M Lyon^{1,3} ✉

¹James Tarpo Jr. and Margaret Tarpo Department of Chemistry, Purdue University, West Lafayette, United States •

²Department of Pharmacology and Toxicology, Medical College of Georgia, Augusta University, Augusta, United States •

³Department of Biological Sciences, Purdue University, West Lafayette, United States • ⁴Center for Clinical and Translational Research, Abigail Wexner Research Institute at Nationwide Children's Hospital, Columbus, United States •

⁵Graduate School of Pharmaceutical Sciences, Tohoku University, Sendai, Japan • ⁶Graduate School of Pharmaceutical

Sciences, Kyoto University, Kyoto, Japan • ⁷Molecular, Cellular and Pharmacobiology Section, Institute for Pharmaceutical Biology, University of Bonn, Bonn, Germany

eLife Assessment

This **important** study combines cryo-EM, biochemical, and cell-based assays to examine how Gβγ interacts with and potentiates PLCβ3. The authors present evidence for multiple Gβγ interaction surfaces and argue that Gβγ primarily enhances PLCβ3 activity after membrane recruitment rather than serving mainly as a membrane-recruitment factor. The evidence is **solid** overall, although uncertainty remains about the physiological relevance and precise arrangement of the proposed interfaces because the structural model relies on engineered crosslinking.

<https://doi.org/10.7554/eLife.110382.1.sa4>

Abstract

Phospholipase C β (PLCβ) enzymes are activated by heterotrimeric G protein subunits, increasing hydrolysis of phosphatidylinositol-4,5-bisphosphate (PIP2) at the plasma membrane. All four human PLCβ isoforms (PLCβ1-4) are activated by Gα_q, while PLCβ1-3 are activated to varying extents by Gβγ. The binding sites for Gα_q on PLCβ are well-established and much has been learned about its mechanism of activation, but comparatively little is known about Gβγ-dependent activation. In this work, we used cryo-electron microscopy (cryo-EM) single particle analysis (SPA), functional assays, and bioluminescence resonance energy transfer (BRET) to investigate how Gβγ interacts with PLCβ3 in concert with activated Gα_q to regulate phospholipase activity. Gβγ heterodimers bind multiple surfaces of PLCβ3 to promote activation but alone do not recruit the enzyme to the plasma membrane. Instead, Gβγ facilitates activation by Gα_q, most likely by reorienting the phospholipase catalytic site at the membrane to maximize PIP2 hydrolysis and downstream Ca²⁺ release. Cell-based functional assays demonstrate that Gβγ is required for maximal PLCβ3 activation even when G_q heterotrimers are the sole source of Gβγ. Together, these findings demonstrate that Gβγ acts as a critical positive allosteric modulator that regularly acts in concert with Gα_q to activate PLCβ3 at the plasma membrane.

Introduction

Heterotrimeric G proteins regulate a wide variety of effectors downstream of G protein-coupled receptors (GPCRs). One family of effector enzymes are the phospholipase Cβ (PLCβ) enzymes. The four PLCβ isoforms (PLCβ1-4) cleave phosphatidylinositol-4,5-bisphosphate (PIP2) to inositol-1,4,5-trisphosphate (IP3) and diacylglycerol (DAG). These second messengers in turn increase

intracellular Ca^{2+} and activate protein kinase C (PKC). All PLC β isoforms are activated by direct binding of $\text{G}\alpha_q$, released by G_q -coupled receptors. PLC β 2, PLC β 3, and to a lesser extent PLC β 1, are also stimulated by binding of $\text{G}\beta\gamma$ heterodimers, released by G_i -coupled receptors (1, 2).

PLC β s share four core domains with other PLC enzymes, including a pleckstrin homology (PH) domain, four EF hands, a catalytic triose phosphate isomerase (TIM) barrel split by a regulatory linker (X–Y linker) into X and Y subdomains, and a C2 domain. The PLC β subfamily is defined by its unique proximal and distal C-terminal domains (CTDs) that follow the C2 domain. The proximal CTD (pCTD) includes the autoinhibitory the Ha2' helix, which is displaced when $\text{G}\alpha_q$ binds (3), and the distal CTD (dCTD), which contributes to membrane binding and contains a second functionally critical $\text{G}\alpha_q$ binding site (2). The mechanism by which $\text{G}\alpha_q$ binds to and activates PLC β has been well characterized through functional and structural studies (3–6), but the mechanism by which $\text{G}\beta\gamma$ activates PLC β is much less clear.

The $\text{G}\beta\gamma$ heterodimer has no intrinsic enzymatic activity yet regulates a wide variety of effector enzymes via membrane recruitment and/or allostery (7, 8). Prior studies of $\text{G}\beta\gamma$ regulation of PLC β identified two potential, non-overlapping binding sites for $\text{G}\beta\gamma$. The first was the PH domain, which serves primarily as a protein-protein interaction site in the PLC β subfamily (9, 10). The PH domain is required for $\text{G}\beta\gamma$ stimulation of PLC β and chimeras of PLC δ that contained the PH domain of PLC β gained sensitivity to the G protein subunit (11). The second $\text{G}\beta\gamma$ binding site was mapped to a helix in the Y subdomain of the TIM barrel. Peptides corresponding to this region blocked $\text{G}\beta\gamma$ activation of PLC β and crosslinked to $\text{G}\beta\gamma$ (12, 13). However, $\text{G}\beta\gamma$ binding to this site appeared to preclude the PLC β active site from engaging the membrane for PIP₂ hydrolysis. The mechanism of $\text{G}\beta\gamma$ -dependent activation is further complicated by reports that, in cells, the process requires prior or coincident activation by $\text{G}\alpha_q$ (14–16).

Recent structural work has shed light onto how $\text{G}\beta\gamma$ interacts with PLC β . Cryo-electron microscopy (cryo-EM) reconstructions of $\text{G}\beta\gamma$ and PLC β on liposomes and nanodiscs showed two $\text{G}\beta\gamma$ molecules bound to one PLC β 3, one to the PH domain and one to the EF hand domain (17). The latter domain had not previously been implicated in $\text{G}\beta\gamma$ -dependent activation. $\text{G}\beta\gamma$ binding did not induce conformational changes within the lipase, and despite its proximity to a lipid bilayer, PLC β 3 remained in its autoinhibited conformation; the active site remained occluded by the X–Y linker and inhibitory interactions between the Ha2' helix and the catalytic core persisted. Because no allosteric changes in the lipase were observed, a model was proposed in which $\text{G}\beta\gamma$ activates PLC β 3 by recruiting it to and orienting it at the plasma membrane (17). Consistent with this idea, the same study demonstrated $\text{G}\beta\gamma$ -dependent partitioning of PLC β 3 to a lipid bilayer (17), although several prior studies using purified components did not show $\text{G}\beta\gamma$ -dependent recruitment of the lipase to membranes (18–20). Additionally, the $\text{G}\beta\gamma$ –PLC β 3 interface(s) responsible for activation in the cellular environment are unknown. Finally, it is also unclear if G protein activation liberates sufficient free $\text{G}\beta\gamma$ to recruit PLC β 3 in cells.

Here we investigate the mechanism by which $\text{G}\beta\gamma$ binding to PLC β 3 increases lipase activity using crosslinking, cryo-EM single particle analysis (SPA), and functional assays in living cells. We report cryo-EM reconstructions of $\text{G}\beta\gamma$ –PLC β 3 that reveal a third binding site for $\text{G}\beta\gamma$ involving the PH, EF hand, and C2 domains. We show that all three structurally determined interfaces contribute to $\text{G}\beta\gamma$ -dependent activation in cells. Notably, we find that free $\text{G}\beta\gamma$ does not promote recruitment of PLC β 3 to the plasma membrane, and that membrane-tethered PLC β 3 can still be activated by $\text{G}\beta\gamma$. Thus, $\text{G}\beta\gamma$ binds to multiple sites on the lipase to further stimulate PIP₂ hydrolysis concomitant with activation of PLC β 3 by $\text{G}\alpha_q$, most likely by orienting the enzyme at the plasma membrane. We propose that $\text{G}\beta\gamma$ is best understood as a critical positive allosteric modulator of PLC β 3, as opposed to a bona fide activator in cells.

Results

Cryo-EM reconstructions of G β γ -PLC β 3 complexes in solution

We first attempted to determine the solution structure of a soluble G β γ -PLC β 3 complex, in which the prenylated Gy C68 is mutated to serine (G β γ C68S) (21), eliminating the need for lipids and/or detergents. Complexes of G β γ C68S-PLC β 3 could be isolated by size exclusion chromatography (SEC) but were too unstable for structural determination, in agreement with previous studies (17). We turned to crosslinking to isolate a stable complex (22). Solvent-exposed cysteines in the lipase (human PLC β 3 residues 193, 221, 358, 516, 824 and 834) were mutated to serines in the background of PLC β 3 Δ 892, a C-terminal truncation which lacks the distal CTD yet retains robust activation by G β γ (23–25). Given the evidence that G β γ binds to the PH domain, an E60C mutation was installed in the PH domain (PLC β 3 Δ 892 PH_{cys}) to facilitate crosslinking with G β γ C68S (G β 1 contains fourteen cysteines, with C204 and C271 solvent-exposed, while Gy2 contains two cysteines with only C68 solvent-exposed). As a control, C516 was retained in the X–Y linker (PLC β 3 Δ 892 XY_{cys}). Neither variant underwent self-crosslinking, in contrast to PLC β 3 Δ 892 which retains the endogenous cysteines, but only PLC β 3 Δ 892 PH_{cys} crosslinked efficiently to G β γ C68S (Figure S1C). Bismaleimidoethane (BMOE), an 8 Å crosslinker had a crosslinking efficiency of >50%, and a 1:1 complex was observed with PLC β 3 Δ 892 PH_{cys}, consistent with a persistent and specific interaction (Figure S1B). To confirm the BMOE-crosslinked G β γ -PLC β 3 Δ 892 PH_{cys} complex was functional, crosslinking was repeated using wild-type G β γ and PLC β 3 Δ 892 PH_{cys}, resulting in ~3-fold greater activity than the reaction without the crosslinker (Figure S1C). Similar results were also obtained with the 14.7 Å BM(PEG)2 crosslinker. The crosslinked G β γ -PLC β 3 Δ 892 PH_{cys} complexes were purified using SEC and subjected to cryo-electron microscopy (cryo-EM) single particle analysis (SPA). Two reconstructions were independently refined to 4 Å and 7 Å resolution in the BMOE data set (Figures 1, S2, S3, Table 1), and one 4.4 Å reconstruction in the BM(PEG)2 data set (Figures S2, S4, Table 1).

In all crosslinked G β γ -PLC β 3 Δ 892 PH_{cys} complexes, G β γ engages PLC β 3 via a surface formed primarily by the PH and EF1/2 domains that differs from the two interfaces observed previously (17). The relative orientation and local resolution of G β γ with respect to PLC β 3 varies in each case, suggesting the interface is conformationally heterogeneous, most likely due to the absence of a membrane (Figure S2). Even though all the cysteines in G β are retained, and both G β C271 and C204 are in the “hotspot” interaction surface of G β γ , only a single crosslink between PLC β 3 E60C and G β Cys271 is observed. In all G β γ -PLC β 3 reconstructions reported, G β C204 is ~25 Å from PLC β 3 E60, well beyond the range of either BMOE or BM(PEG)2. There are also no solvent-exposed cysteines in G β γ at the EF hand binding site within ~45 Å of PLC β 3 E60. This is consistent with a specific, persistent interaction that results in the crosslink between G β 271 and PLC β 3 E60C. Indeed, density for the crosslinker is observed in the 4 Å BMOE reconstruction, and the orientation of G β γ and PLC β 3 in the 7 Å BMOE and BM(PEG)2 reconstructions are also consistent with crosslinking via this site.

In the crosslinked complexes, as in the prior structures, PLC β 3 Δ 892 PH_{cys} is autoinhibited by its X–Y linker and pCTD (Figure 1) (3, 4, 9, 17, 26). This is consistent with previous reports demonstrating the membrane is essential for regulation by G β γ and that its activation mechanism is independent of the PLC β CTDs (2). The crosslinked G β γ is situated such that it allows simultaneous binding of G α_q to PLC β with the C-terminal helix of Gy nearly in the same plane as the phospholipase active site. Thus, the solution reconstruction may represent a membrane-localized complex, but not a catalytically active state.

In the 4 Å reconstruction (Figures 1, 2A), the G β γ -PLC β 3 Δ 892 PH_{cys} interface buries ~1,400 Å² surface area. This is more extensive than the G β γ -PH domain or G β γ -EF hand interfaces, which bury ~800 Å² and ~1,100 Å² respectively (Figures 2B, 2C) (17). The primary G β γ interface is formed by residues on the side of the WD40 toroid, rather than its face, which is the typical effector interface. Nevertheless, the crosslinked G β γ -PLC β 3 Δ 892-PH_{cys} interface includes several residues known to be critical for enzyme activation, and the specific interactions differ from the other reported G β γ -PLC β 3 interfaces. In the BMOE complex, G β D228 interacts with R199 and

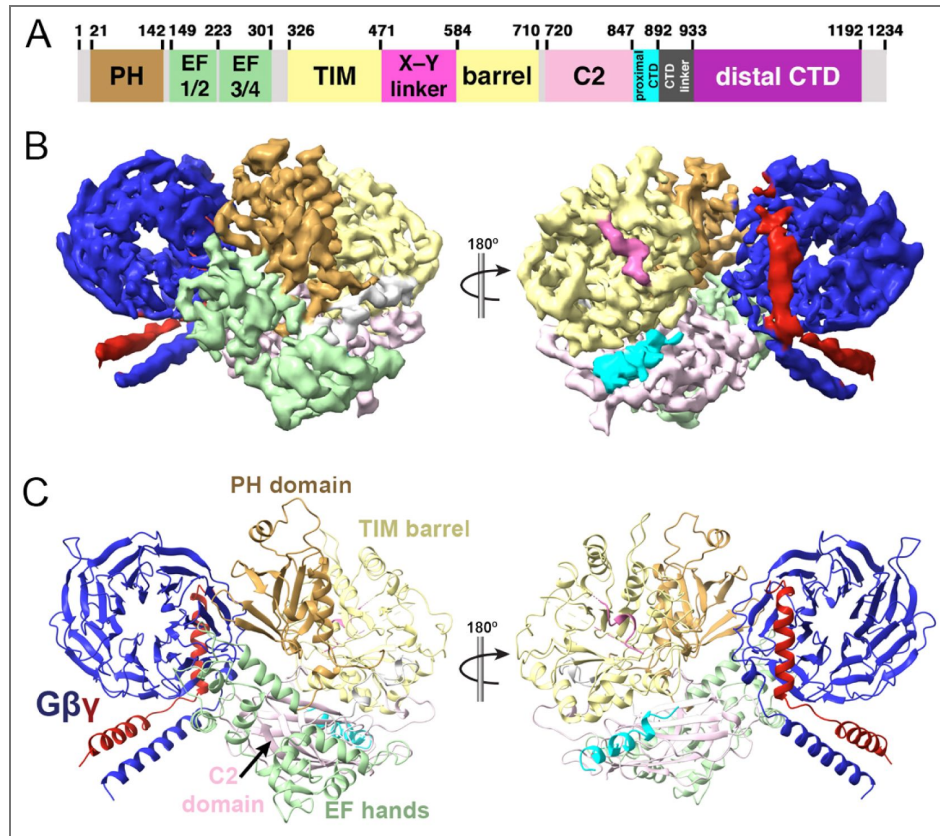


Figure 1. Cryo-EM reconstruction of the Gβγ-PLCβ3 Δ892-PH_{cys} complex

(A) Domain diagram of human PLCβ3, with numbers above corresponding to domain boundaries. PLCβ3 is regulated by the X-Y linker (hot pink), proximal C-terminal domain (CTD, cyan), and distal CTD (purple). The CTDs are connected by the unconserved CTD linker. (B) Cryo-EM density map and (C) structure of the 4 Å Gβγ-Δ892-PH_{cys} complex crosslinked with BMOE, with PLCβ3 colored as in 1A, Gβ in blue, and Gγ in red.

	Gβγ-PLCβ3 BMOE (4.1 Å)	Gβγ-PLCβ3- BMOE (7.0 Å)	Gβγ-PLCβ3 BMPEG
Data collection and processing			
Grids	Cu Quantifoil	Cu Quantifoil	Cu Quantifoil
Vitrification Method	FEI Vitrobot	FEI Vitrobot	FEI Vitrobot
Microscope	Titan Krios	Titan Krios	Titan Krios
Magnification	81000	81000	81000
Voltage (kV)	300	300	300
Detector	K3	K3	K3
Electron exposure (e ⁻ /Å ²)	53.69	53.69	53.69
Defocus range (μm)	0.5-2.0	0.5-2.0	0.5-2.0
Pixel size (Å)	0.539	0.539	0.539
Frames	40	40	40
Symmetry	C1	C1	C1
Micrographs			
Initial particle images (no.)	1,248,953	1,248,953	579,743
Final particle images (no.)	92,777	65,306	142,175
Map resolution (Å)	4.06	6.77	4.40
FSC threshold	0.143	0.143	0.143
Refinement			
Initial model used (PDB code)	4GNK (PLCβ3)	4GNK (PLCβ3)	4GNK (PLCβ3)
	1GP2 (Gβ _{1γ2})	1GP2 (Gβ _{1γ2})	1GP2 (Gβ _{1γ2})
Model resolution (Å)	4.06	6.77	4.40
FSC threshold	0.143	0.143	0.143
Model resolution range (Å)	3.4-7.0	7-10.7	4-10.7
Model composition			
Non-hydrogen atoms	8,913	8,896	8,967
Protein residues	1,125	1,125	1134
Ligands	8	0	0
B factors (Å ²)			
Protein	74.40	45.30	55.51
Ligand	79.08	0	0
R.m.s. deviations			
Bond lengths (Å)	0.003	0.002	0.003
Bond angles (°)	0.474	0.542	0.519
Validation			
MolProbity score	1.97	2.61	2.98
Clashscore	6.37	11.34	40.75
Poor rotamers (%)	1.64	4.71	3.35
Ramachandran plot			
Favored (%)	92.9	90.75	91.80
Allowed (%)	6.92	9.25	8.02
Disallowed (%)	0.18	0	0.18

Table 1. Cryo-EM data collection, refinement and validation statistics

K183 in PLC β 3, whereas in the G β γ -PLC β 3-G β γ reconstruction G β D228 interacts with R24 or K238 in the PH domain and EF hand interfaces, respectively (Figure 2A-C). In our G β γ -PLC β 3 Δ 892 PH_{cys} structure, G β K301 and R304 on blade 6 make electrostatic interactions with PLC β 3 D655 and E34, respectively (Figure 2A). These interactions were not reported in the liposome-bound G β γ -PLC β -G β γ complex (17), and provide a structural explanation for observations reported over thirty years ago by Neer and coworkers on the importance of G β blades 6 and 7 in lipase activation (27, 28). On the other hand, G β W99, a critical residue for effector activation including PLC β 2 (29), does not interact with the lipase in the crosslinked complexes, but does interact in the G β γ -PLC β 3-G β γ complex. Taken together with previous structural findings, our results suggest that G β γ can bind to PLC β 3 at several sites with modest affinity.

Functional analysis of G β γ -PLC β 3 interfaces: IP accumulation

To assess the functional relevance of the G β γ -PLC β 3 interfaces observed in cryo-EM reconstructions (Figure 2) we carried out cell-based inositol phosphate (IP) accumulation assays in COS7 cells, where PLC β 3 is increased by the overexpression of either G β γ or G α_q . Mutations of residues in PLC β 3 or G β γ at any one of the three observed interfaces decreased G β γ -dependent activation of the lipase (Figures 2D-G). PLC β 3 mutants with decreased responsiveness to G β γ are most likely impaired in binding the G β γ heterodimer, as their expression and activation by G α_q were minimally altered (Figures 2D-G; Figure S5). PLC β 3 K183E, which eliminates an electrostatic interaction with G β E226 and D228 in the crosslinked complexes, has 3-fold lower G β γ -stimulated activity (Figures 2D,E), as do PLC β 3 R24E, L40G, and R185L, which disrupt interactions with G β γ observed in the liposome-tethered reconstructions (Figure 2E) (17, 29). G β D228R, which interacts with PLC β 3 in all reconstructions (Figures 2F, G) (17, 30), decreased activation of PLC β 3 by \sim 20-fold, which cannot be fully attributed to reduced protein expression (Figure S5). Mutations in G β blades 6 and 7, G β K301E and R304D, also decreased PLC β 3 activation, in agreement with previous reports (23) (Figure 2F,G).

Functional analysis of G β γ -PLC β 3 interfaces: PLC β 3 interaction with G β γ

Under physiological conditions, PLC β 3 is activated in response to GPCR stimulation that activates G α_q heterotrimers, rather than overexpression of G α_q or G β γ , as in the previous experimental setting. To assess the functional significance of the three G β γ -PLC β 3 interfaces downstream of receptor activation we developed a BRET assay to monitor G β γ binding to PLC β 3 in live cells in real time. This effort was complicated by the fact that a large fraction of PLC β 3 is cytosolic, whereas G β γ is anchored to the plasma membrane. Because of this, recruitment of PLC β 3 to the plasma membrane by any means (e.g. binding to G α_q ·GTP) would cause an increase in bystander BRET between PLC β 3 and G β γ that would sum with BRET due to direct interactions between the two. To eliminate this confound, we anchored HiBit-labeled PLC β 3 to the plasma membrane with a C-terminal CAAX motif, which prevents increases in bystander BRET due to translocation and thus isolates signals due to interactions between Venus-G β γ and the lipase at the plasma membrane. Activation of angiotensin AT $_1$ receptors induced a rapid increase in BRET between HiBit-PLC β 3-CAAX (coexpressed with LgBit and G α_q) and Venus-G β γ (Figure 3A). This signal was completely blocked by membrane-localized GRK3ct, which binds and sequesters free G β γ , and enhanced by membrane-localized GRK2RH, which binds and sequesters free G α_q ·GTP (Figure 3A). The latter observation is complementary to our previous finding that sequestering G β γ enhances G α_q binding to PLC β 3; both findings suggest that PLC β 3 competes with G protein subunits for binding to the complementary G protein subunits (6).

We next used this interaction assay to test a series of fifteen HiBit-PLC β 3-CAAX mutants designed to disrupt the three structurally determined G β γ -PLC β 3 interfaces. Mutations in the two interfaces observed in the liposome-tethered reconstructions significantly reduced agonist-induced BRET between Venus-G β γ and HiBit-PLC β 3-CAAX (Figure 3B). For example, L40E in the PH domain interface and R185E in the EF hand interface almost completely abolished receptor-mediated signals (Figure 3B). In contrast, K183E in the crosslinked complex interface did not significantly

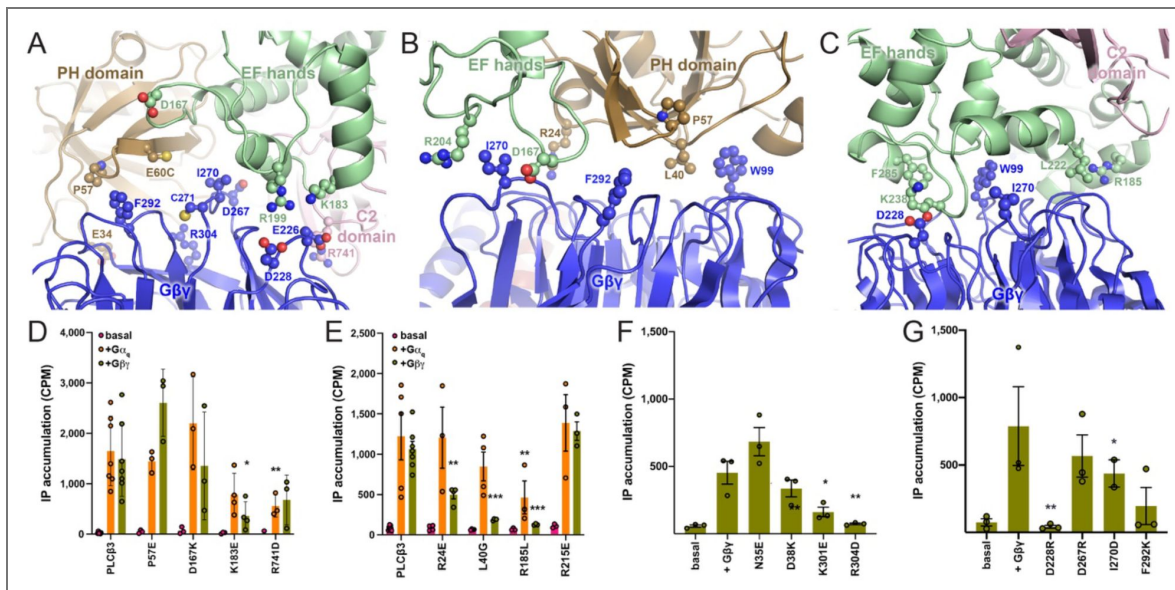


Figure 2. Functional analysis of Gβγ-PLCβ3 interfaces: IP accumulation.

Comparison of the (A) Gβγ-Δ892-PH_{cys} interface observed in this study, and the previously reported (B) Gβγ-PLCβ3 PH and (C) Gβγ-PLCβ3 EF hand interfaces (PDB ID: 8EMW) (17). Proteins are colored as in Fig. 1. Residues in PLCβ3 and Gβγ shown as balls and sticks were mutated, and their basal and G protein-dependent activities quantified in a cell-based [³H]-IP_x accumulation assay. Gα_q-dependent activation was used as a control to confirm the PLCβ3 variants were properly folded. Changes in activity are not due to differences in expression (Figure S3). The activities of the PLCβ3 mutants in the (D) BMOE-crosslinked Gβγ-Δ892-PH_{cys} interface and (E) Gβγ-PLCβ3 PH/EF hand interfaces were measured. Mutations to the Gβ₁ subunit were similarly assessed for (F) the crosslinked Gβγ-Δ892-PH_{cys} interface and (G) the Gβγ-PH/EF hand interfaces. All assays were performed in triplicate from at least three independent transfections, and data shown are mean ± SEM. Data in D and E were analyzed using a two-way ANOVA followed by Dunnett's post-hoc multiple comparisons test, comparing the basal activity of each PLCβ3 variant to its activation Gβγ or Gα_q. ***, p<0.0005, **, p<0.005, *, p<0.05. Data in F and G were analyzed using a one-way ANOVA, followed by Dunnett's post-hoc multiple comparisons test, comparing each the Gβγ-stimulated activity of each PLCβ3 mutant to wild-type PLCβ3. ***, p<0.0005, **, p<0.005, *, p<0.05.

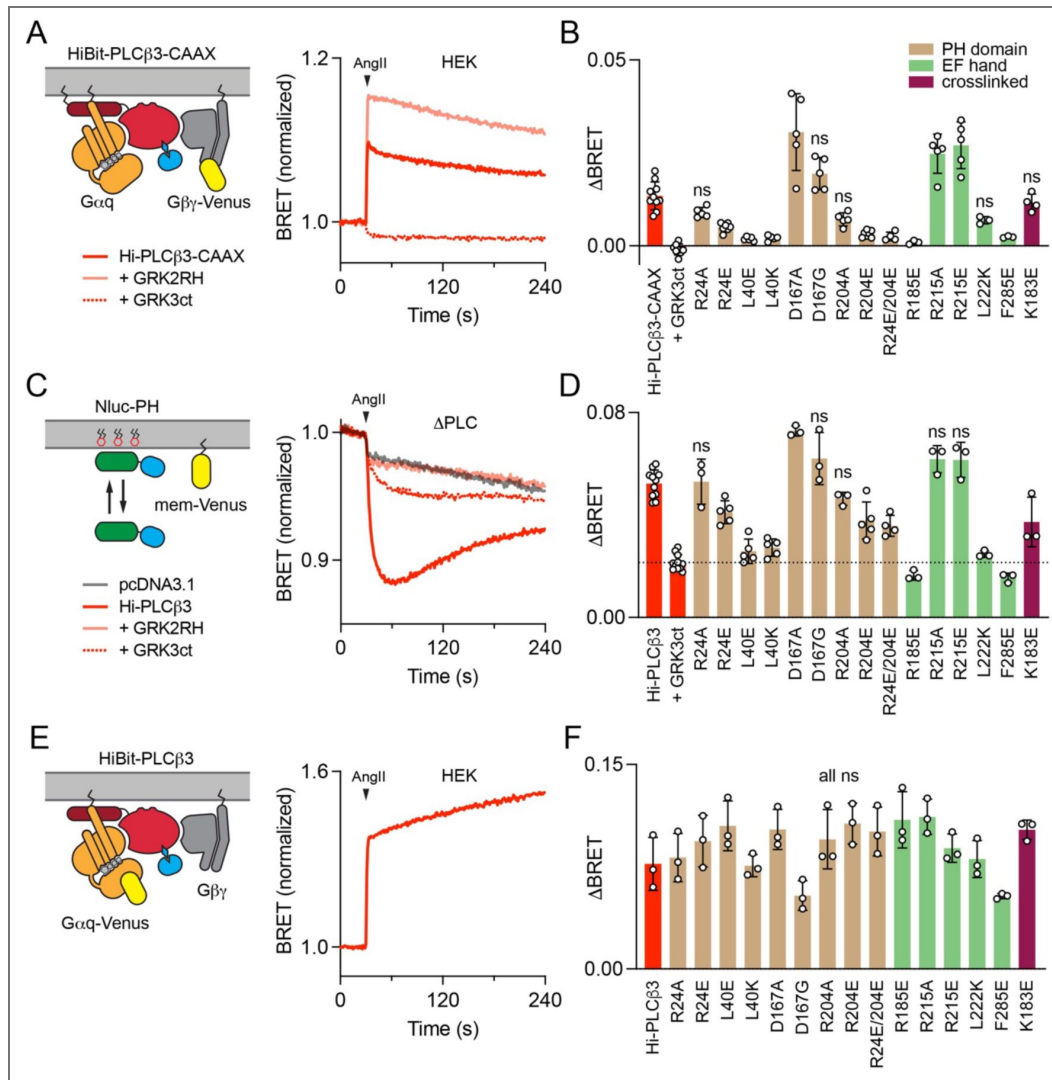


Figure 3. Functional analysis of Gβγ-PLCβ3 interfaces: interaction with G proteins and PIP hydrolysis.

(A) BRET between membrane-anchored HiBit-PLCβ3-CAAX and Venus-Gβγ increases after activation of AT₁ with angiotensin II (AngII; 1 μM). Signals are blocked by mem-GRK3ct (GRK3ct), and enhanced by membrane associated GRK2RH, which sequester free Gβγ and Gα_q-GTP, respectively. Traces are the average of twenty replicates from five independent experiments. (B) AngII-induced changes in BRET between HiBit-PLCβ3-CAAX and Venus-Gβγ (ΔBRET) for fifteen mutants across the three Gβγ-PLCβ3 interfaces; most mutants showed significant changes in interaction with Venus-Gβγ compared to wild-type HiBit-PLCβ3-CAAX. (C) In ΔPLC cells, expression of HiBit-PLCβ3 (without LgBit) reconstitutes AngII-induced PIP₂ hydrolysis, indicated by bystander BRET between Nluc-PH and mem-link-Venus (mem-Venus). Traces are the average of sixteen replicates from four independent experiments. (D) AngII-induced PIP₂ hydrolysis (ΔBRET) for the same HiBit-PLCβ3 mutants as panel B; most mutants showed significant changes in PIP₂ hydrolysis. (E) In HEK cells BRET between HiBit-PLCβ3 and Gα_q-Venus increases after activation of AT₁. Traces are the average of twelve replicates from three independent experiments. (F) BRET between the same HiBit-PLCβ3 mutants as panel B and Gα_q-Venus; none of the mutants showed significant changes compared to wild-type HiBit-PLCβ3. For B, D, and F all mutants were compared to wild-type HiBit-PLCβ3-CAAX or HiBit-PLCβ3 using one-way ANOVA with Dunnett's post-hoc comparisons; data points represent averages from independent experiments (n=3-11) performed in quadruplicate. Only non-significant (ns; defined as p>0.05) mutants are indicated, and individual p values are given in *SI Appendix*, Tables S3-5.

reduce agonist-induced BRET signals, even though this mutation significantly impaired activation by $G\beta\gamma$ in our IP accumulation assays. This is likely due to the position of the Venus BRET acceptor in the crosslinked complex, which is much less conducive to energy transfer from the donor (HiBit + LgBit) to the PLC β 3 N-terminus than the Venus BRET acceptors in the liposome-tethered complexes. Therefore, this assay may be unable to detect $G\beta\gamma$ -PLC β 3 interactions at the crosslinked site. Surprisingly, mutations at residues D167 in the PH domain interface and R215 in the EF hand interface significantly *increased* receptor-mediated interaction between Venus- $G\beta\gamma$ and HiBit-PLC β 3-CAAX (Figure 3B). Overall, these results support the conclusion that the functional defects observed in our IP accumulation assays reflect loss of $G\beta\gamma$ binding.

Notably, the almost complete loss of agonist-induced BRET signals after disruption of either of the PH or EF hand interfaces suggests that, when attached to a membrane, $G\beta\gamma$ dimers might cooperate to bind at both sites. This is consistent with the relatively weak binding of $G\beta\gamma$ *in vitro* and difficulties isolating stable $G\beta\gamma$ -PLC β 3 complexes in solution. We then asked if cooperative binding of G protein subunits might extend to $G\alpha_q$, i.e. if binding of $G\alpha_q$ promotes binding of $G\beta\gamma$. Using the same $G\beta\gamma$ -PLC β 3 interaction assay, we first compared signals downstream of AT $_1$, which activates both G_q and $G_{i/o}$ heterotrimers, to those downstream of the dopamine D2 receptor (D2R), which activates only $G_{i/o}$ heterotrimers. D2R-mediated signals were detectable, but significantly smaller than AT $_1$ -mediated signals (Figure S6A). Under the same conditions, D2R liberated more free Venus- $G\beta\gamma$ than AT $_1$ when detected by the memGRK3ct-Nluc sensor (Figure S6B), suggesting that the presence of $G\alpha_q$ -GTP promotes $G\beta\gamma$ binding to HiBit-PLC β 3-CAAX. To further test this idea we constructed HiBit-PLC β 3-CAAX mutants with disrupted $G\alpha_q$ binding to the proximal CTD (HiBit-PLC β 3-CAAX-LE) or the distal CTD (HiBit-PLC β 3-CAAX-EEE) (6). Interaction of both mutants with Venus- $G\beta\gamma$ was significantly impaired compared to wild-type HiBit-PLC β 3-CAAX (Figure S6C). These results suggest that $G\beta\gamma$ binding to the PH and EF interfaces is facilitated by binding of $G\alpha_q$ -GTP.

Functional analysis of $G\beta\gamma$ -PLC β 3 interfaces: receptor-evoked PIP2 hydrolysis

To better understand the role of $G\beta\gamma$ binding to different interfaces in receptor-mediated PLC β 3 activation, we carried out PIP2 hydrolysis assays based on binding of the PH domain of PLC δ to PIP2 at the plasma membrane. PIP2 hydrolysis releases Nluc-PH-PLC δ (Nluc-PH) into the cytosol, which is detected as a loss of bystander BRET to a marker on the plasma membrane (mem-Venus; Figure 3C). We first established that endogenous $G\beta\gamma$ contributes to activation of endogenous PLC β 3 (the only PLC β isoform expressed at significant levels in HEK 293 cells) downstream of AT $_1$ receptors. Accordingly, PIP2 hydrolysis after activation of AT $_1$ was inhibited by GRK3ct (Figure S7A, B). Because AT $_1$ receptors activate both G_q and $G_{i/o}$ heterotrimers, we were interested to know the source of the $G\beta\gamma$ contributing to PLC β 3 activation. We found that pertussis toxin (PTX) partially blocked AT $_1$ -mediated PIP2 hydrolysis, consistent with $G\beta\gamma$ from $G_{i/o}$ heterotrimers stimulating lipase activity (Figure S7A, B). However, GRK3ct still inhibited PIP2 hydrolysis when PTX was present, indicating $G\beta\gamma$ from G_q heterotrimers contributes as well (Figure S7A, B).

Next, we reconstituted the same PIP2 hydrolysis assay in genome-edited HEK 293 cells lacking endogenous PLC β proteins (Δ PLC cells) by expressing wild-type (wt) or mutant HiBit-PLC β 3. PIP2 hydrolysis mediated by expressed HiBit-PLC β 3 was inhibited by GRK3ct to roughly the same extent as that mediated by endogenous PLC β 3 in parental cells (Figure 3C). Notably, PIP2 hydrolysis under these conditions was completely blocked by GRK2RH, consistent with the idea that activation of PLC β 3 by $G\beta\gamma$ in cells requires $G\alpha_q$ -GTP (Figure 3C). PIP2 hydrolysis signals mediated by HiBit-PLC β 3 variants with impaired $G\beta\gamma$ binding were significantly smaller than signals mediated by wt HiBit-PLC β 3 (Figure 3D). Among the most defective variants were the L40E PH domain and R185E EF hand mutants, the latter supporting very modest PIP2 hydrolysis comparable to that remaining when $G\beta\gamma$ is sequestered by GRK3ct (Figure 3D). Consistent with our $G\beta\gamma$ sequestration results, both of these mutants were still significantly impaired in the presence of PTX (Figure S7C, D). In agreement with our IP accumulation assays, K183E in the crosslinked complex interface significantly reduced agonist-induced PIP2 hydrolysis (Figure

3D [↗](#)). Conversely, in agreement with our G $\beta\gamma$ interaction results, the D167A mutant in the PH domain interface significantly *increased* receptor-mediated PIP2 hydrolysis (Figure 3D [↗](#)). Overall, there was an excellent correlation between G $\beta\gamma$ binding and PIP2 hydrolysis across the fifteen mutants we tested, and good agreement with our IP accumulation assays. There were no significant differences between wt HiBit-PLC β 3 and any mutant with respect to association with G α_q -Venus (Figure 3E, F [↗](#)) or expression level (*SI Appendix, Table S1* [↗](#)), ruling out indirect effects on G α_q binding or protein stability. These findings indicate that all three of the structurally resolved G $\beta\gamma$ -PLC β 3 interfaces contribute to activation of PLC β 3 downstream of AT $_1$ receptors.

G $\beta\gamma$ facilitates activation of membrane-anchored PLC β 3

PLC β 3 is not tightly anchored to the plasma membrane, and G $\beta\gamma$ has been proposed to increase lipase activity by recruiting the holoenzyme to the membrane. We previously found that AT $_1$ activation results in recruitment of PLC β 3 to the plasma membrane, but concluded that this was primarily mediated by binding to G α_q -GTP (6). To test the possibility that G $\beta\gamma$ binding contributes to membrane recruitment of PLC β 3, we used our previously established bystander BRET recruitment assay (Figure 4A [↗](#)). We found that none of the mutations that inhibited Venus-G $\beta\gamma$ binding and PIP2 hydrolysis significantly impaired recruitment of HiBit-PLC β 3 to the plasma membrane (Figure 4B [↗](#)), indicating that recruitment depends entirely on binding to G α_q -GTP (6). As an alternative test of this hypothesis, we asked if G $\beta\gamma$ increased the activity of HiBit-PLC β 3-CAAX, which is tightly anchored to the plasma membrane and therefore not subject to translocation from the cytosol. We found that GRK3ct was effective at inhibiting PIP2 hydrolysis mediated by HiBit-PLC β 3-CAAX (Figure 4C [↗](#)), similar to its effect on PIP2 hydrolysis mediated by endogenous PLC β or HiBit-PLC β 3. Likewise, mutations in HiBit-PLC β 3-CAAX that impaired G $\beta\gamma$ binding also impaired PIP2 hydrolysis (Figure 4C, D [↗](#)). Taken together, these results suggest that G $\beta\gamma$ does not facilitate PLC β 3 activation by recruiting the lipase to the plasma membrane, but rather enhances the catalytic activity of G α_q -bound PLC β 3 through a distinct allosteric mechanism at the membrane.

Discussion

PLC β enzymes have critical roles in numerous processes, from cardiovascular and vascular smooth muscle function to opioid sensitivity (31–35). PLC β basal activity is tightly controlled, and direct binding of G α_q and G $\beta\gamma$ subunits, released downstream of G $_q$ - and G $_{i/o}$ -coupled receptors, is essential for robust PIP2 hydrolysis (2). The mechanisms by which G α_q interacts with PLC β to increase lipase activity have been well-characterized through structural and functional studies (2, 3, 5, 6, 36). Much less is known about how G $\beta\gamma$ binds to and activates PLC β 1-3. Prior studies established roles for the PH domain and, to a lesser extent, the TIM barrel in G $\beta\gamma$ -dependent activation (11–13, 18, 22, 37). The cryo-EM structure of a liposome-tethered G $\beta\gamma$ -PLC β 3 complex confirmed that G $\beta\gamma$ bound directly to the PH domain, and surprisingly, that a second G $\beta\gamma$ molecule bound to the EF hands (17). However, the functional relevance of both binding sites remained unclear. Moreover, binding of G $\beta\gamma$ also failed to induce conformational changes in the lipase necessary for activation, despite the proximity to a membrane surface. A model was proposed in which G $\beta\gamma$ activates PLC β 3 via membrane recruitment and orientation (17). However, this model contradicted previous studies showing G $\beta\gamma$ did not recruit PLC β to the plasma membrane (12, 18, 22, 25, 38–40). Thus, the question of mechanism remained unsettled.

In this study, we used cryo-EM, activity and signaling assays, and BRET to validate G $\beta\gamma$ -PLC β 3 interactions, assess their contribution to PIP2 hydrolysis, and establish whether G $\beta\gamma$ activates PLC β 3 via membrane recruitment. Using cryo-EM, we identified a third G $\beta\gamma$ binding site on the PLC β 3 PH domain and confirmed all structurally determined G $\beta\gamma$ binding sites are necessary for maximum G protein-stimulated activity (Figures 1 [↗](#)–3 [↗](#)). Multiple G $\beta\gamma$ subunits binding to a single effector is not without precedent, as two G $\beta\gamma$ molecules must bind to non-overlapping sites on phosphatidylinositol 3-kinase γ (PI3K γ) for maximum membrane recruitment and activation (41, 42). The structures of G $\beta\gamma$ -PLC β 3 complexes all tether the lipase to the membrane (Figure 5 [↗](#)), but it is unlikely that all three sites could be occupied simultaneously during catalysis. In the

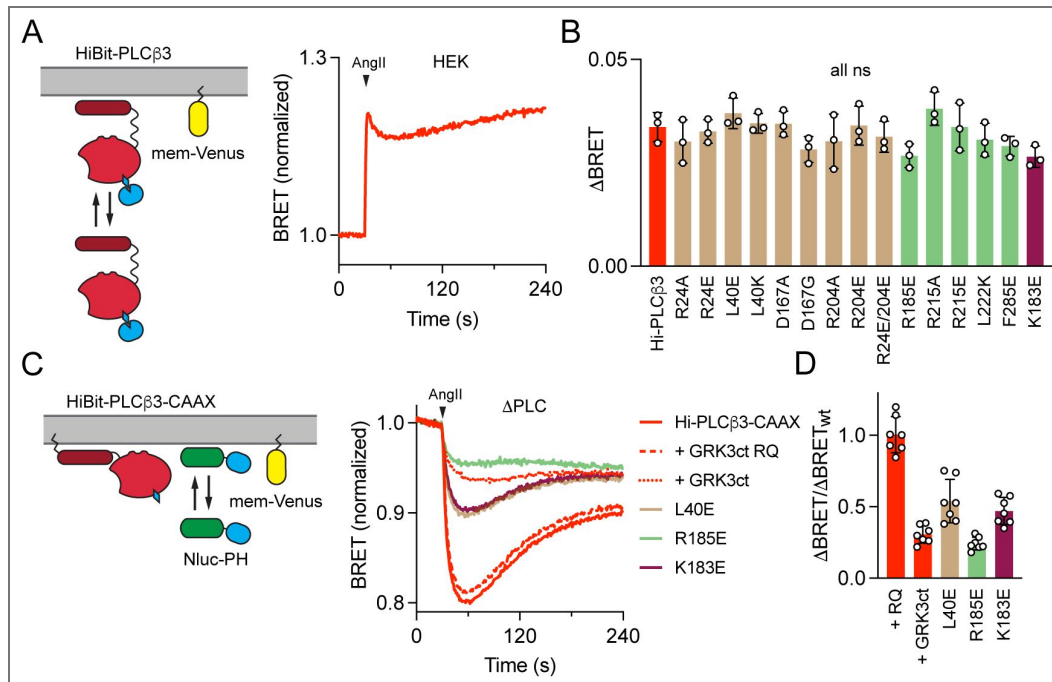


Figure 4. Gβγ facilitation of PLCβ3 activation does not reflect membrane recruitment.

(A) Activation of AT₁ induces translocation of HiBit-PLCβ3 to the plasma membrane as indicated by bystander BRET between HiBit-PLCβ3 and mem-Venus. Traces are the average of twelve replicates from three independent experiments. (B) BRET between the same HiBit-PLCβ3 mutants as Figure 3 and mem-Venus; none of the mutants showed a significant defect in membrane translocation compared to wild-type HiBit-PLCβ3; individual p values are given in *SI Appendix, Table S6*. (C) In ΔPLC cells, expression of HiBit-PLCβ3-CAAX reconstitutes AngII-induced PIP₂ hydrolysis, indicated by bystander BRET between Nluc-PH and mem-Venus. Signals are inhibited by GRK3ct, which sequesters free Gβγ. Traces are the average of twenty-eight replicates from seven independent experiments. (D) PLCβ3-CAAX variants shown to be defective with respect to Gβγ binding are also defective with respect to PIP₂ hydrolysis. For B, all mutants were compared to wild-type HiBit-PLCβ3, and for D all mutants were compared to +GRK3ct RQ using one-way ANOVA with Dunnett's post-hoc comparisons; data points represent averages from independent experiments (*n*=3 or 7) performed in quadruplicate. Only non-significant (ns; defined as *p*>0.05) mutants are indicated, and individual p values are given in *SI Appendix, Tables S6-7*.

crosslinked G $\beta\gamma$ -PLC β 3 complex, the orientation of G $\beta\gamma$ is unlikely to be compatible with the binding of the lipase active site to the membrane (Figures 1 [↗](#), 5A [↗](#)). We propose this reflects an encounter complex, or pre-activation state, given the specificity and efficiency of the crosslinking reaction (Figure S1 [↗](#)). In contrast, both G $\beta\gamma$ molecules in the liposome-tethered G $\beta\gamma$ -PLC β 3 complex and the lipase active site can simultaneously interact with the membrane (Figure 5B [↗](#)). Our observation that disruption of either of these sites can severely compromise G $\beta\gamma$ binding suggests a degree of cooperativity between these sites.

Comparisons of the predicted G $\beta\gamma$ binding sites in PLC β 1-4 provide some insights into the isoform-specific differences in G $\beta\gamma$ -dependent activation. Of the nine residues we identified as functionally relevant across the three PLC β 3 G $\beta\gamma$ binding sites (Figures 2 [↗](#), 3 [↗](#)), only two are conserved in PLC β . The other residues are incompatible with G $\beta\gamma$ binding and explain why G $\beta\gamma$ does not activate PLC β 4 (43, 44). In PLC β 1 and PLC β 2, seven of the residues identified are conserved, the exceptions being PLC β 3 R204 and R215. In PLC β 1, these residues are replaced by proline and valine, respectively, and in PLC β 2 they are asparagine and serine. Whether these differences are sufficient to explain why PLC β 1 is weakly activated by G $\beta\gamma$ while PLC β 2 is robustly activated remains to be established (1).

Previous work has shown that PLC β 3 must be preactivated, or simultaneously activated, by G α_q -GTP in cells before G $\beta\gamma$ binds to further increase PIP2 hydrolysis (14). This is consistent with the fact that all G $\beta\gamma$ -PLC β 3 reconstructions are fully compatible with simultaneous binding G α_q -GTP at the membrane (Figure 5C, D [↗](#)). G α_q binding is essential for translocation of the lipase to the plasma membrane (6), but mutation of any of the three structurally characterized G $\beta\gamma$ binding sites has no impact on lipase translocation (Figure 3 [↗](#)). Moreover, free G $\beta\gamma$ released by activation of G $\gamma_{1/0}$ heterotrimers does not promote translocation (6). While G $\beta\gamma$ clearly does not increase lipase activity via membrane recruitment, its binding to the lipase is essential for maximum PIP2 hydrolysis (Figure 3 [↗](#)), even when PLC β 3 is tethered at the membrane (Figure 4 [↗](#)). While G $\beta\gamma$ recruitment and reorientation of PLC β 3 at the membrane were proposed as activation mechanisms, they were not directly tested. Here, we have elucidated this mechanism, and our results demonstrate that G $\beta\gamma$ is a positive allosteric modulator of PLC β 3, following direct activation of the phospholipase by G α_q , as opposed to a *bona fide* activator. In this paradigm, G $\beta\gamma$ binding to the PH domain and/or EF hands optimizes the orientation of G α_q -PLC β 3 at the membrane to facilitate interfacial activation and maximize PIP2 hydrolysis (Figure 5E [↗](#)).

Finally, our results show that G $\beta\gamma$ is surprisingly important for PLC β 3 activation by G α_q heterotrimers in cells. While synergistic activation of PLC β 3 by G α_q and G $\beta\gamma$ is well known, this synergy is typically discussed as a mechanism of crosstalk between G α_q and G α_i signaling, the latter being the source of G $\beta\gamma$ dimers (45, 46). G $\beta\gamma$ affinity for PLC β 3 is relatively low and only G $\gamma_{1/0}$ heterotrimers are thought to be expressed at high enough levels to release sufficient free G $\beta\gamma$. Here we show that PIP2 hydrolysis downstream of G α_q alone is sensitive to sequestration of G $\beta\gamma$ dimers, consistent with a previous study in HeLa cells (47), as well as mutations that disrupt G $\beta\gamma$ binding. Endogenous G α_q heterotrimers are evidently capable of releasing sufficient free G $\beta\gamma$ to occupy binding sites on PLC β 3. This is most likely enabled by cooperative binding of G protein subunits to PLC β 3 at the plasma membrane.

Materials and Methods

Cell culture and transfection

Human embryonic kidney HEK 293 cells were obtained from ATTC (CRL-1573) and used as supplied or after gene editing as described previously (15, 58); Δ PLC β 1-4 (Δ PLC) cells were generated using CRISPR/Cas9 and validated as described previously (15). Cells were transfected in 6-well plates in growth medium using linear polyethyleneimine MAX (Polysciences) at a nitrogen/phosphate ratio of 20 and were used for experiments 24-48 hours later. Up to 3.0 μ g of plasmid DNA was transfected in each well of a 6-well plate. COS-7 cells were a gift from A.V. Smrcka and used for [3 H]-IP $_x$ accumulation assays.

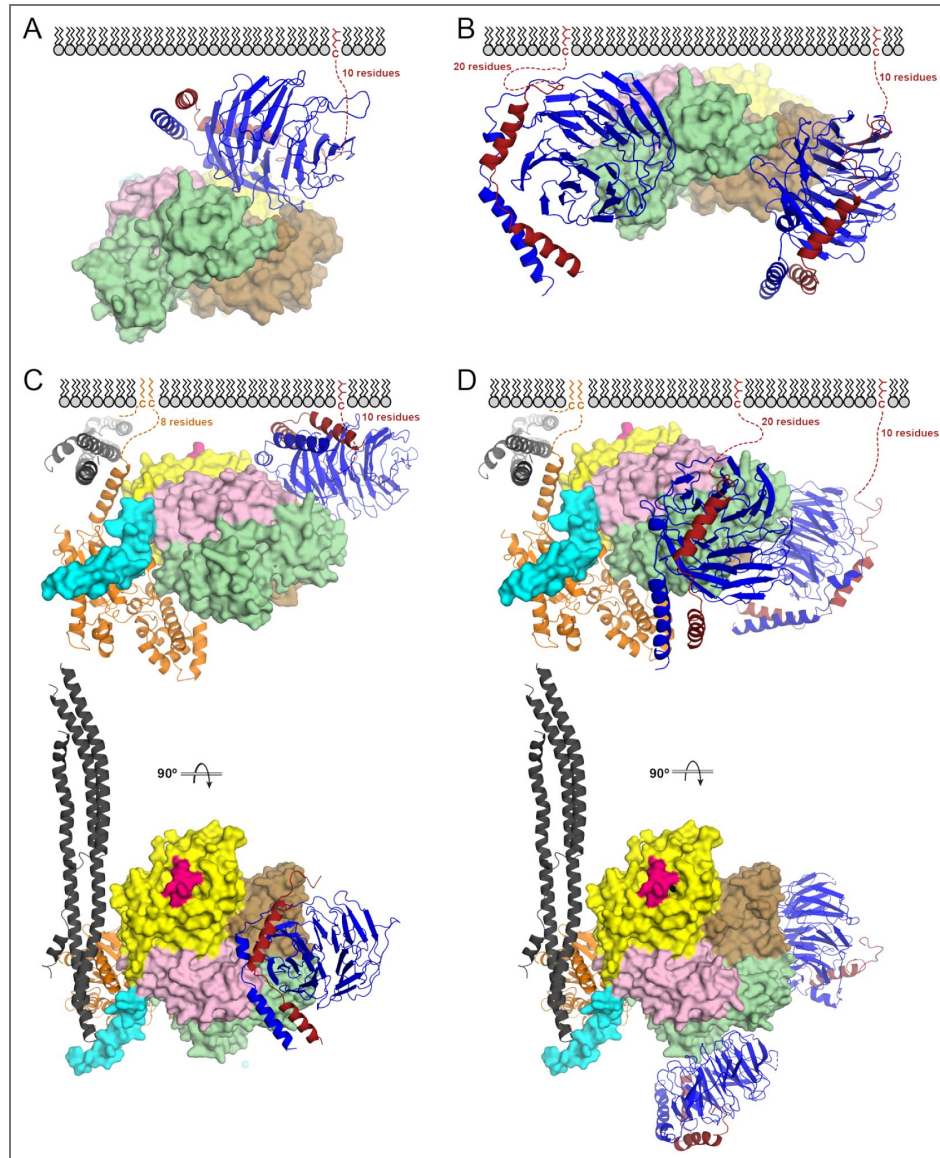


Figure 5. G protein-PLC β 3 complexes at the membrane.

(A) The crosslinked G β γ -PLC β 3 complex is compatible with membrane localization, but not lipase activity. PLC β 3 is shown as a surface, and G β γ in ribbon. Proteins are colored as in Fig. 1A. (B) The liposome-tethered G β γ - PLC β 3 complex would allow the PLC β 3 active site to interact with the membrane. (C) The crosslinked and (D) liposome-tethered complexes are compatible with G α_q -GTP binding and activation via displacement of the H α 2' helix (cyan) and engagement of the dCTD (dark gray). In both models, the dCTD binds the membrane through electrostatic interactions.

Plasmids

SNAPf-AGTR1, HiBit-PLC β 3, HiBit-PLC β 3-CAAX, mem-link-Venus, mem-GRK3ct, mem-link-amber-GRK2RH, Nluc-PH, Gaq-Venus, CMV-LgBit, Venus-1-155-G γ 2 and Venus-156-239-G β 1 were described previously (6). Mutations in HiBit-PLC β 3, HiBit-PLC β 3-CAAX were made by amplifying three fragments from wild-type plasmids with the desired mutation incorporated in a primer, assembling using Gibson assembly and verifying by full plasmid sequencing. Mutations in human PLC β 3 in pFastbac1, pCMV, or pCDNA3.1 were generated using the Takara infusion site-directed mutagenesis kit (Takara) (Supplemental Table 1) and verified by full plasmid sequencing. The same strategy was used to subclone G β 1 and G γ 2 in pCI-Neo(59) and Gaq in pCDNA3.1+.

Protein expression, purification, and complex formation

Protein expression

PLC β 3, PLC β 3 Δ 892 and variants, G $\beta\gamma$, and G $\beta\gamma$ C68S were expressed and purified from baculovirus-infected insect cells. Baculoviruses were generated using the FastBac recombinant baculovirus system (Invitrogen/Thermo Fisher Scientific, Inc.) in ESF 921 Insect Cell Culture Medium (Expression Systems)-adapted Sf9 (*Spodoptera frugiperda*) cells.

Purification of G $\beta\gamma$ and G $\beta\gamma$ C68S

High Five cells were infected with baculoviruses encoding His6-Ga α 1, G β 1, and G γ 2 (49, 60). Cells were harvested 60 h post-infection by centrifugation at 2,500 x g, frozen in liquid N $_2$ and stored at -80 °C.

All purification steps were performed at 4 °C unless otherwise indicated. Cell pellets were thawed in 15 mL of lysis buffer (50 mM HEPES pH 8.0, 3 mM MgCl $_2$, 10 mM β -mercaptoethanol, 0.1 mM EDTA, 100 mM NaCl, 10 μ M GDP, and protease inhibitors (133 μ M PMSF, 21 μ g/mL TLCK, and 0.5 μ g/mL TPCK) and lysed by four freeze-thaw cycles in liquid nitrogen. Lysate was diluted to 100 mL with lysis buffer and centrifuged at 100,000 x g for 30 min to isolate the membrane fraction. The membrane pellets were resuspended by dounce in 5 mL extraction buffer (50 mM HEPES pH 8.0, 3 mM MgCl $_2$, 50 mM NaCl, 10 mM β -mercaptoethanol, 10 μ M GDP, and protease inhibitors), combined and diluted to 60 mL. Cholate was added to a final concentration of 1% and the mixture stirred for 1 h at 4 °C to extract membrane proteins. Detergent extracts were clarified by centrifugation at 100,000 x g for 45 min. The supernatant was diluted five-fold with buffer A (50 mM HEPES pH 8.0, 3 mM MgCl $_2$, 10 mM β -mercaptoethanol, 100 mM NaCl, 10 μ M GDP, 0.5% polyoxyethylene(10) lauryl ether (C12E10), and protease inhibitors) and applied to a cOmplete™ His-Tag Purification Resin (Roche) column pre-equilibrated with buffer A. The column was washed with 100 mL of buffer A supplemented with 300 mM NaCl and 5 mM imidazole, then transferred to room temperature and washed with 12 mL buffer A. G β 1 γ 2 subunits were released from His6-Ga α 1 using six 4 mL fractions of RT buffer (buffer A supplemented with 150 mM NaCl, 5 mM imidazole, 50 mM MgCl $_2$, 10 mM NaF, 10 μ M AlCl $_3$, and 1% cholate). Fractions were analyzed by SDS-PAGE and Coomassie staining to assess purity. Fractions containing G $\beta\gamma$ were pooled and applied to a MonoQ column pre-equilibrated with 20 mM HEPES, pH 8, 1 mM DTT, 50 mM NaCl and 0.5% CHAPS, and eluted with a 50-500 mM NaCl gradient. Fractions containing purified protein were identified by SDS-PAGE, concentrated to 20-40 μ M, flash frozen in liquid N $_2$, and stored at -80 °C.

G $\beta\gamma$ C68S was purified as described with some modifications. Briefly, after cell lysis, the supernatant was diluted five-fold with buffer A lacking polyoxyethylene(10) lauryl ether, glass fiber-filtered, and applied to cOmplete™ His-Tag Purification Resin (Roche) as described. The rest of the steps were carried out as described, with the omission of cholate or CHAPS from the buffers.

Purification of PLC β 3 and variants

His6-PLC β 3, PLC β 3 Δ 892, PLC β 3 Δ 892-PH $_{cys}$ and PLC β 3 Δ 892-XY $_{cys}$ were expressed in Sf9 insect cells grown in S6900 II serum-free media and infected with baculovirus at an MOI of 1(52). After 48 h, cells were harvested by centrifugation, frozen in liquid N $_2$ and stored at -80°C. Cells were rapidly thawed and lysed by four freeze-thaw cycles in liquid nitrogen in lysis buffer (20 mM HEPES, pH 8, 50 mM NaCl, 10 mM β -mercaptoethanol, 0.1 mM EDTA, 0.1 M EGTA, 133 μ M PMSF, 21

$\mu\text{g/ml}$ TLCK and TPCK, 0.5 $\mu\text{g/ml}$ aprotinin, 0.2 $\mu\text{g/ml}$ Leupeptin, 1 $\mu\text{g/ml}$ Pepstatin A, 42 $\mu\text{g/ml}$ Tosyl-L-Arginine Methyl Ester (TAME), 10 $\mu\text{g/ml}$ Soy Bean Trypsin Inhibitor (SBTI) Lysed cells were collected and diluted with lysis buffer and NaCl to a final concentration of 800 mM NaCl, and centrifuged at $100,000 \times g$ for 1 h. The supernatant was diluted 5 fold with lysis buffer containing 0.5% polyoxyethylene(10) lauryl ether (C12E10) and centrifuged again at $100,000 \times g$ for 1 h The supernatant was loaded onto a cOmplete™ His-Tag Purification Resin (Roche) column pre-equilibrated with buffer A (20 mM HEPES, pH 8, 100 mM NaCl, 10 mM β -mercaptoethanol, 0.1 mM EDTA, and 0.1 M EGTA). The column was washed with 3 column volumes (CVs) of buffer A, followed by 3 CVs of buffer A supplemented with 300 mM NaCl and 10 mM imidazole. The protein was eluted with 3-10 CVs of buffer A supplemented with 200 mM imidazole. Proteins were concentrated and loaded onto tandem Superdex 200 columns (10/300 GL; GE Healthcare) equilibrated with SEC buffer (20 mM HEPES pH 8, 200 mM NaCl, 2 mM DTT, 0.1 mM EDTA, and 0.1 M EGTA). Fractions containing purified protein were identified by SDS-PAGE and were pooled, concentrated, and flash frozen in liquid N_2 .

Crosslinking and complex isolation

Purified $\text{G}\beta\gamma$ -C68S, $\text{G}\beta\gamma$, $\text{PLC}\beta 3 \Delta 892$, $\text{PLC}\beta 3 \Delta 892\text{-PH}_{\text{cys}}$, and $\text{PLC}\beta 3 \Delta 892\text{-XY}_{\text{cys}}$ were buffer exchanged to remove DTT by concentrating the proteins in an Amicon Ultra 0.5 ml 30 K concentrator (Millipore-Sigma) and washing them twice with 20 mM HEPES pH 7.4, 100 mM NaCl, 0.1 mM EDTA and 0.1 mM EGTA (and 0.5% CHAPS for $\text{G}\beta\gamma$). 25 μM of the buffer-exchanged $\text{G}\beta\gamma$ and 25 μM $\text{PLC}\beta 3 \Delta 892$, $\text{PLC}\beta 3 \Delta 892\text{-PH}_{\text{cys}}$ or $\text{PLC}\beta 3 \Delta 892\text{-XY}_{\text{cys}}$ were mixed and crosslinking initiated by addition of 200 μM BMOE or BMPEG2. Reactions were incubated for 45 min at room temperature and quenched by addition of 20 mM DTT. Crosslinking of $\text{G}\beta\gamma$ and $\text{PLC}\beta 3 \Delta 892\text{-PH}_{\text{cys}}$ were completed as above but contained 0.5% CHAPS. Crosslinking was confirmed by SDS-PAGE by the presence of a band at ~ 135 kDa, consistent with a 1:1 stoichiometric complex ($\text{G}\beta$ MW: 35 kDa, $\text{PLC}\beta 3 \Delta 892$ MW: 100.89 kDa)

Cryo-EM

Sample preparation and data collection

For the BMOE-crosslinked and BM(PEG)2-crosslinked $\text{G}\beta\gamma$ C68S– $\text{PLC}\beta 3 \Delta 892\text{-PH}_{\text{cys}}$ complexes, 3.5 μL of purified complex at 1 mg/mL supplemented with 0.2 % CHAPS_(f) ~ 5 min before blotting was applied onto glow-discharged Quantifoil R1.2/1.3 300-mesh grids and prepared and imaged as described for $\text{PLC}\beta 3$. For the BMOE sample, Micrographs were collected on a Titan Krios G1 electron microscope (FEI) equipped with a post-GIF K3 direct electron detector (Gatan) in the Purdue Life Science Cryo-EM facility. A dataset containing $\sim 4,515$ images was collected in super-resolution mode with a pixel size of 0.539 Å, at a defocus range of 1-3 μm using Leginon. For each movie stack, 40 frames were recorded at a frame rate of 78 ms per frame and a total dose of 53.69 electrons/Å². Micrographs were collected on a Titan Krios G4 electron microscope (FEI) equipped with a Post-GIF K3 direct electron detector (Gatan) in the Purdue Life Science Cryo-EM facility. A dataset containing $\sim 4,587$ images was collected in super-resolution mode with a pixel size of 0.539 Å, at a defocus range of 1-3 μm using EPU. For each movie stack, 40 frames were recorded at a frame rate of 78 ms per frame and a total dose of 53.43 electrons/Å².

Data processing

Micrographs were motion aligned and motion corrected using motioncor2 (61) implemented within CryoSPARC(53). CTF estimations were completed using CTFFind4 (62). Particle picking, 2D classifications, initial model generation, 3D classification and refinement were all performed using CryoSPARC. Workflows for each data set are shown in Figures S4 (63), S5 (63), and S6 (63). The nominal resolution was determined based on a Fourier shell correlation cutoff of 0.143.

Model building and refinement

Crystal structures of $\text{G}\beta\gamma$ and $\text{PLC}\beta 3$ (PDB IDs 1GP2 and 4GNK, (5, 63)) were rigid-body fit into the cryo-EM map using Chimera (64). The model was then refined using molecular dynamic flexible fitting (MDFF)(54). MDFF configuration files were generated using VMD. During MDFF simulation,

G β y was set as rigid with domain restraints. The MDFF simulation was conducted with a grid scaling value of 0.5 for 100 ps, followed by 3,000 steps of energy minimization until convergence of the protein RMSD. The MDFF generated model was inspected and manually adjusted in COOT(55), guided through the use of deep-learning-based amino-acid-wise model quality (DAQ) scoring (65, 66) and refined in PHENIX(56). Resulting models were assessed in PHENIX for stereochemical correctness. Maps, half maps, and coordinate files were deposited in the PDB as 9Y7H, 9YAO, and 9YAP and in the EMDB as EMD-72655, EMD-72732, and EMD-72733.

Activity assays

Inositol phosphate accumulation

COS-7 cells were seeded in 12-well culture dishes at a density of 100,000 cells per well and maintained in Dulbecco's modified Eagle's medium containing 10% fetal bovine serum (Atlanta Bio), 1X Glutamax (Gibco), 100 units/mL penicillin, and 100 μ g/mL streptomycin (Corning) at 37 °C and 5% CO₂. Cells were transfected with 400 ng of PLC β 3 variant and 200 ng G protein subunit using Fugene 6 (Promega) at a 3:1 ratio per manufacturer's protocol. Total DNA varied from 700-900 ng per well, with pCMV used as an empty vector. 18-24 h after transfection, the media was changed to low-inositol Ham's F-10 medium (Gibco) containing 1.5 μ Ci/well myo-[2-³H(N)] inositol (Perkin Elmer) for 16-18 h, then treated with 10 mM LiCl for 1 h to inhibit inositol phosphatases. Media was aspirated, cells were washed twice with PBS, then lysed by addition of ice-cold 50 mM formic acid. Lysates containing [³H]-inositol phosphate were applied to Dowex AGX8 columns to isolate the IP species. Columns were washed twice with 10 CVs of 50 mM formic acid, then 100 mM formic acid, and eluted with 3 CVs of 1.2 M ammonium formate into scintillation vials containing scintillation fluid and counted.

Western blotting

Cells were lysed in SDS sample buffer (100 mM Tris pH 6.8, 6% sucrose, 2% SDS, 715 mM β -mercaptoethanol, and 0.02% bromophenol blue), boiled, and run on a 10% (w/v) SDS-polyacrylamide gel. Proteins were transferred to PDVF for 16 hours at 25 V, followed by incubation with an antibody against PLC β 3 (Cell Signaling Cat: D9D6S) (1:1000), G β 1 (Thermo: Cat: PA530046) or actin (Cell Signaling: 8H10D10) (1:2000). Goat anti-rabbit HRP or goat anti-rabbit AlexaFlour 800 antibodies (1:10,000) were added before visualizing with ECL reagent (Pierce) for HRP linked antibodies. Western blots were imaged with a GeneGnome imaging system or Azure Sapphire FL respectively.

Liposome-based activity assay

Hen egg white phosphatidylethanolamine (PE) at 100 μ M and soy phosphatidylinositol (PI) at 250 μ M (Avanti Polar Lipids) were resuspended in CHCl₃, mixed, and dried in 312 μ L aliquots in borosilicate glass tubes under N₂, sealed and stored at -20 °C until use. To prepare liposomes, the lipids were resuspended in 312 μ L of sonication buffer (50 mM HEPES pH 7, 80 mM KCl, 2 mM EGTA, and 1 mM DTT) and incubated at room temperature for 5 min, then sonicated to clarity in 30 second duty cycles using a bath sonicator (Avanti Polar Lipids). Each reaction mixture contained 10 μ L of liposome solution, 10 μ L of PLC solution (50 mM HEPES pH 7, 3 mM EGTA, 80 mM KCl, 3 mM DTT, and 3 mg/mL BSA), 5 μ L of G β y solution or buffer (50 mM HEPES pH 7, 100 mM NaCl, 5 mM MgCl, 1 mM DTT, and 3 mM EGTA), and 5 μ L of CaCl₂ solution (50 mM HEPES pH 7, 3 mM EGTA, 80 mM KCl, 1 mM DTT, and 18 mM CaCl₂). CaCl₂ solution was added last to initiate PI hydrolysis upon transfer to 30°C and incubated for 15 minutes. Control reactions contained all components except CaCl₂. Reactions were terminated by the addition of an ice-cold quench solution (50 mM HEPES pH 7, 80 mM KCl, 210 mM EGTA, and 1 mM DTT), and incubated on ice.

Inositol phosphate (IP) was quantified using a modified version of the CisBio IP-One Gq assay kit. Following termination, 14 μ L of each reaction mixture, 3 μ L of d2-labeled IP1, and 3 μ L of the cryptate-labeled anti-IP1 antibody (CisBio) were added to a 384-well low-volume white microplate at room temperature (Corning, Corning, NY). Positive controls contained assay buffer, d2-labeled IP1, and cryptate-labeled anti-IP1, and negative controls contained assay buffer, lysis and detection buffers, and cryptate-labeled anti-IP1. The plate was centrifuged at 1000 x g for 1 min,

incubated at room temperature for 1 h, and fluorescence read on a SynergyNeo2 plate reader (BioTek). The concentration of IP1 was calculated from a standard curve and normalized following the manufacturer's protocol (CisBio).

BRET

For Venus-G β y interaction experiments HEK 293 cells were transfected with 0.01 μ g HiBit-PLC β , 0.1 μ g CMV-LgBit, 0.4 μ g G α_q , 0.3 μ g Venus-1-155-G γ 2, 0.3 μ g Venus-155-239-G β 1 and 0.3 μ g SNAPf-AGTR1. For G α_q -Venus interaction experiments G α_q -Venus replaced G α_q , and unlabeled G β 1 and G γ 2 replaced their Venus-labeled counterparts. For PIP2 hydrolysis assays HEK cells were transfected with 0.01 μ g Nluc-PH, 0.1 μ g SNAPf-AGTR1 and 0.8 μ g of mem-link-Venus. For PIP2 hydrolysis reconstitution assays Δ PLC cells were transfected with the same components plus 0.01 μ g of HiBit-PLC β , HiBit-PLC β -CAAX or variants thereof. To sequester either active G α_q or G β y GRK2RH or GRK3ct were added at 0.2 μ g per well, respectively. For translocation bystander BRET experiments HEK293 cells were transfected with 1 μ g mem-link-Venus, 0.1 μ g CMV-LgBit, 0.3 μ g SNAPf-AGTR1, 0.4 G α_q and 0.01 μ g HiBit-PLC β or variant. Cells were washed and resuspended in Dulbecco's phosphate buffered saline (DPBS) and distributed to 96-well plates in suspension immediately before taking BRET measurements. All BRET measurements were made in the presence of furimazine (Promega or ChemShuttle; 1:1,000 as supplied or from a 5 mM stock dissolved in 90% ethanol/10% glycerol). BRET and luminescence measurements were made using a Polarstar Optima or Lumistar Omega plate reader (BMG Labtech); angiotensin II was injected from a 10-fold concentrated solution. Raw BRET signals were calculated as the emission intensity at 520–545 nm divided by the emission intensity at 475–495 nm. Net BRET signals were calculated as the raw BRET signal minus the raw BRET signal measured from cells expressing only the donor.

Statistical analysis

All analysis was carried out using GraphPad Prism Version 10.5.0.

Materials availability

All unique materials produced for this study are available from the corresponding author upon request.

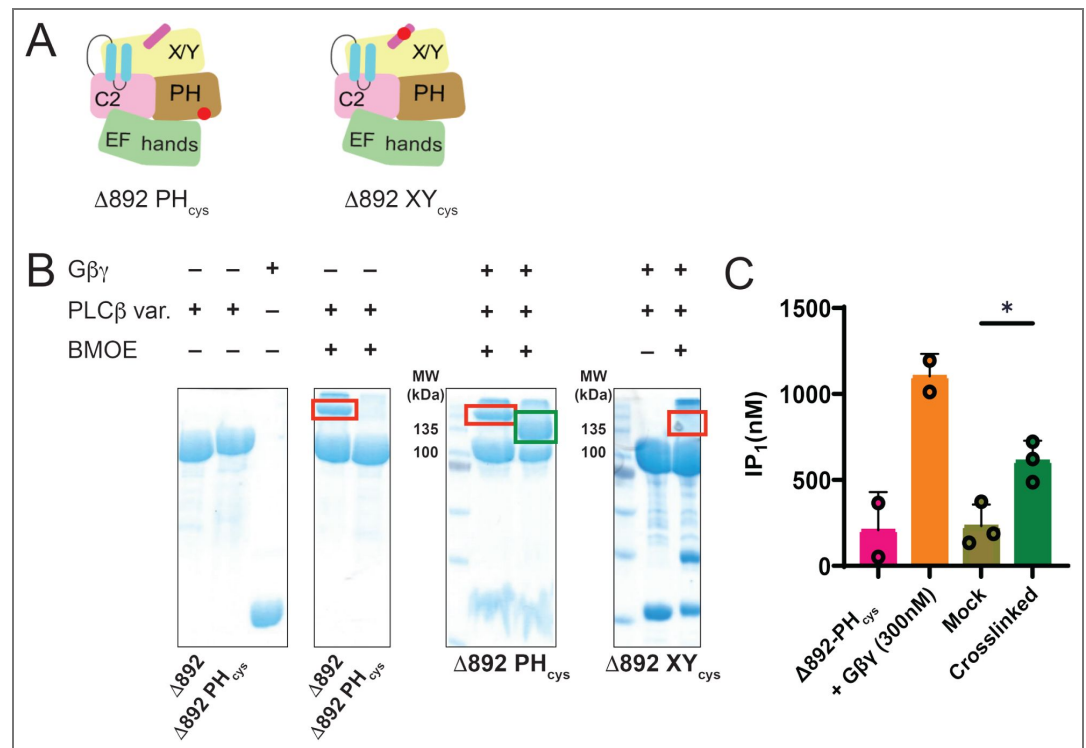


Figure S1. Isolation of a Crosslinked and Functional Gβγ-PLCβ3 complex. (A) Schematic of PLCβ3 Δ892 variants used for crosslinking studies. (B) Representative crosslinking experiments with Gβγ C68S and PLCβ3 Δ892 variants analyzed by SDS-PAGE. PLCβ3 Δ892 undergoes extensive self-crosslinking (red box, left). Mutation of solvent-exposed cysteines and installation of a single cysteine in the PH domain (E60C) eliminates self-crosslinking and allows crosslinking between Gβγ C68S and PLCβ3 Δ892_{PH} (green box). PLCβ3 Δ892_{XY}, which lacks solvent-exposed cysteines with the exception of C516 in the flexible X-Y linker eliminated self-crosslinking but failed to crosslink to Gβγ-C68S. (C) BMOE-crosslinked complexes between wild-type Gβγ and PLCβ3 Δ892_{PH} have higher activity in a liposome-based assay than the uncrosslinked control. Data shown are mean of three separate experiments ± SD. Mock crosslinked and crosslinked samples were compared using an unpaired T-test. *, p < 0.05.

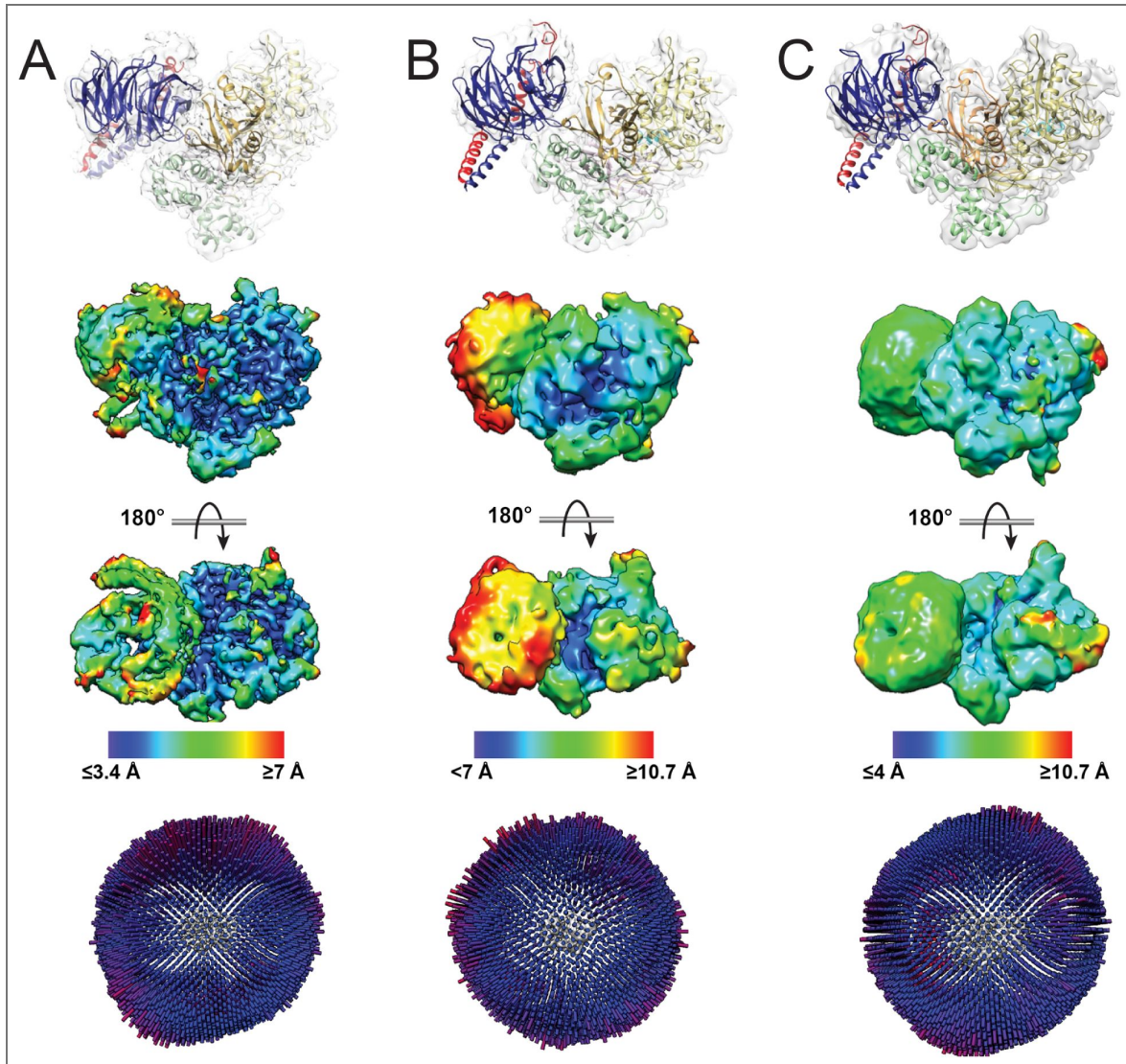


Figure S2. Cryo-EM densities of Gβγ-PLCβ3 Δ892-PH_{cys} complexes.

(A) *Top.* Model of the larger particle population in the BMOE-crosslinked Gβγ-PLCβ3 Δ892-PH_{cys} reconstruction fit into the cryo-EM density map. *Bottom.* Cryo-EM map colored by local resolution. (B) Model of the smaller particle population in the BMOE-crosslinked Gβγ-PLCβ3 Δ892-PH_{cys} reconstruction fit into the cryo-EM density map. *Bottom.* Cryo-EM map colored by local resolution. (C) *Top.* Model of the BM(PEG)2-crosslinked Gβγ-PLCβ3 Δ892-PH_{cys} reconstruction fit into the cryo-EM density map. *Bottom.* Cryo-EM map colored by local resolution. In all reconstructions, resolution is lower for Gβγ, consistent with a dynamic interface in solution.

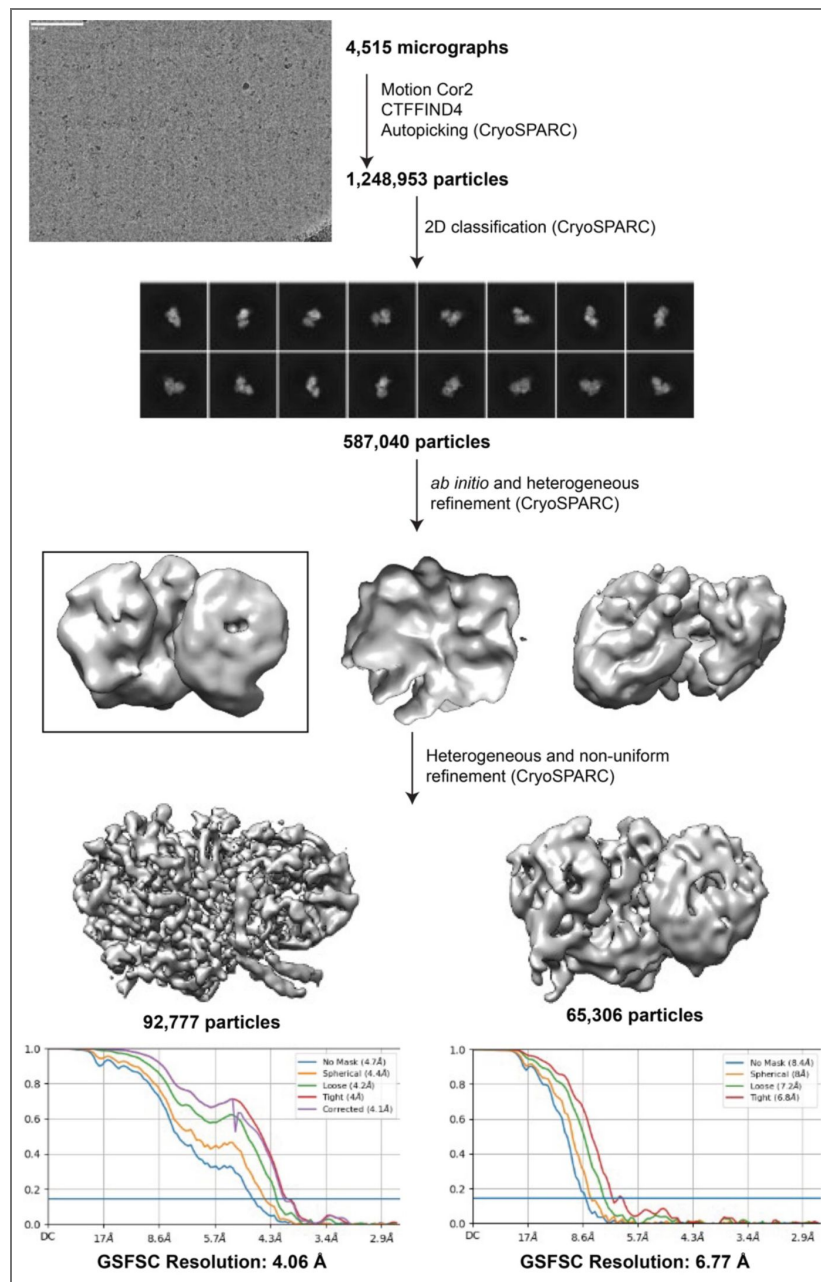


Figure S3. Cryo-EM data workflow and resolution analysis of the BMOE-crosslinked Gβγ- PLCβ3 Δ892-PH_{cys} complex.

The workflow, including a representative micrograph, 2D class averages (box size: 276 Å) and Fourier shell correlation (FSC) curves calculated from two independent reconstructions by CryoSPARC(53). The nominal resolution of the resulting map, as defined by the 0.143 cutoff, is indicated by the horizontal blue line.

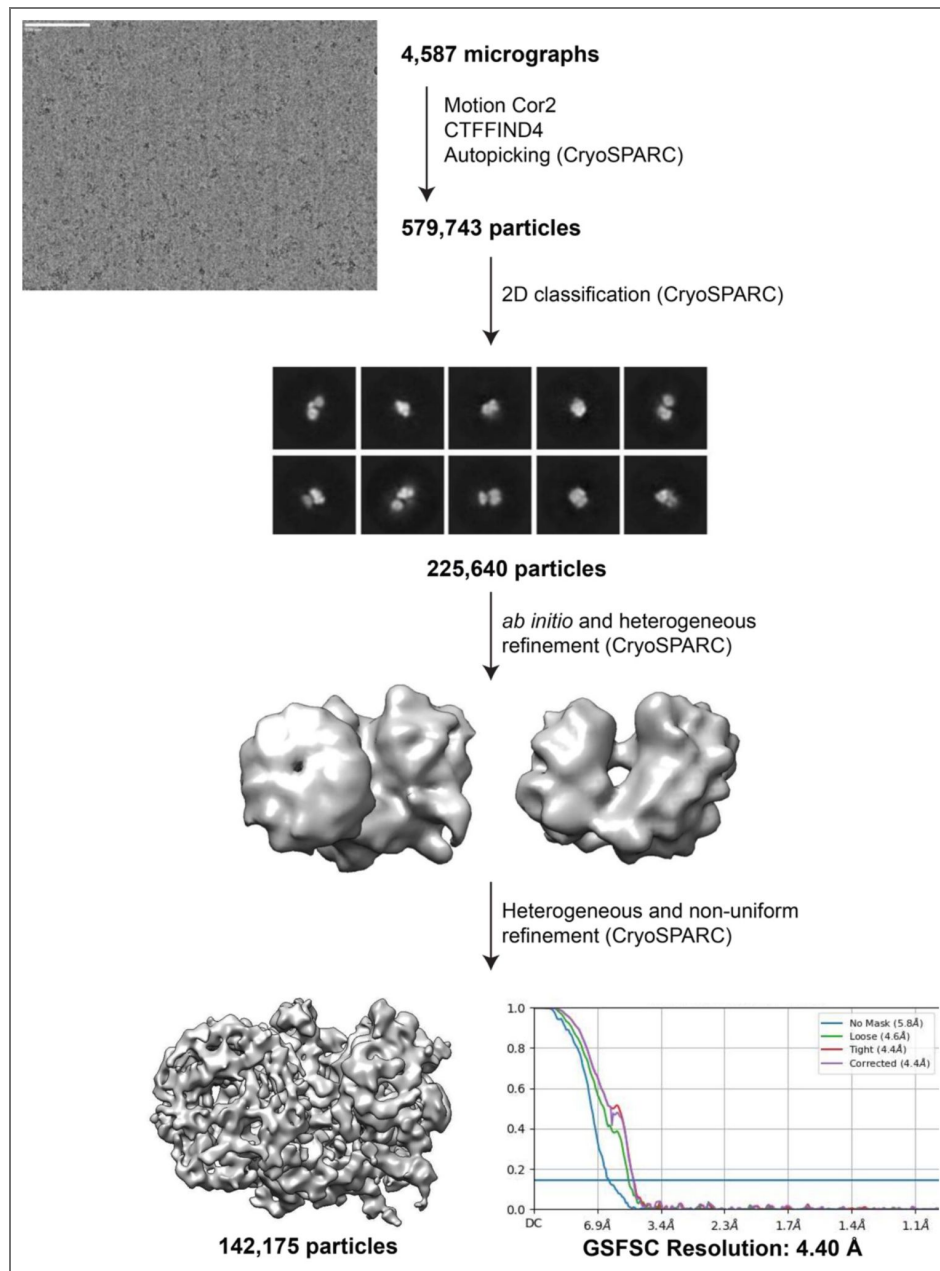


Figure S4. Cryo-EM data workflow and resolution analysis of the BMPEG-crosslinked G β γ -PLC β 3 Δ 892-PH_{cys} complex.

The workflow, including a representative micrograph, 2D class averages (box size: 276 Å) and Fourier shell correlation (FSC) curves calculated from two independent reconstructions by CryoSPARC(53). The nominal resolution of the resulting map, as defined by the 0.143 cutoff, is indicated by the horizontal blue line.

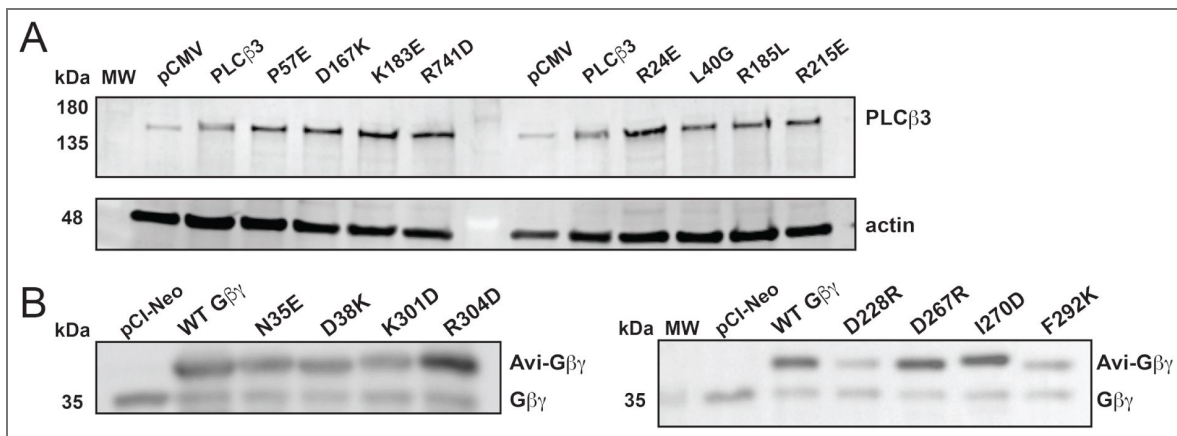


Figure S5. Expression of PLC β 3 and G β 1 mutants.

Representative western blot image of cell lysates containing mutants of interest. **(A)** Western blot image of PLC β 3 point mutants. **(B)** Western blot image of G β 1 mutants. Transfected G β 1 is Avi-tagged (avi-G β 1) and endogenous G β 1 is detected in the untransfected controls.

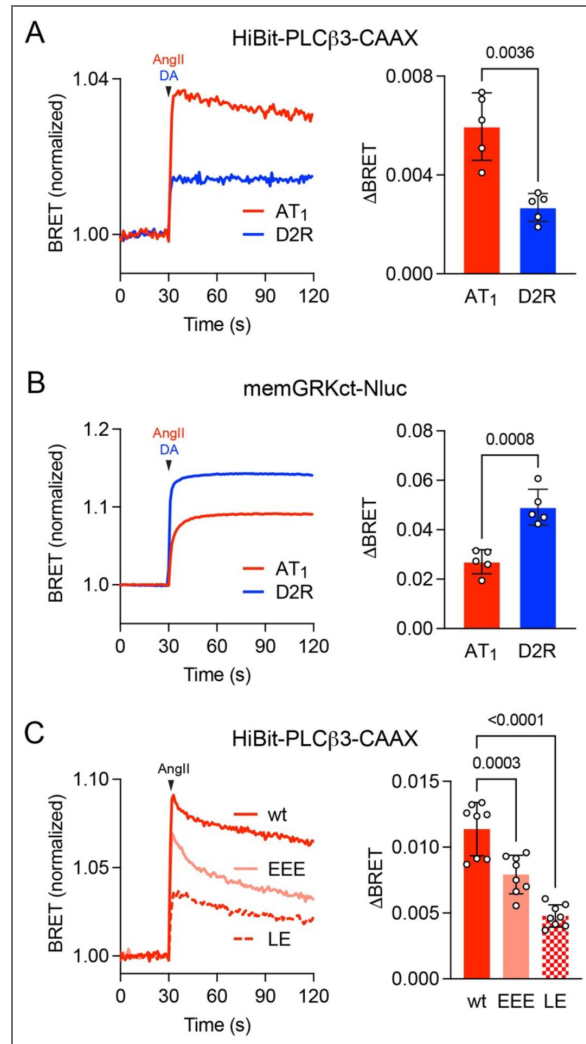


Figure S6. G_{α_q} binding promotes $G\beta\gamma$ binding to PLC β_3 .

(A) BRET between membrane-anchored HiBit-PLC β_3 -CAAX and Venus- $G\beta\gamma$ increases after activation of AT₁ with angiotensin II (AngII; 1 μ M) or dopamine D2R receptors with dopamine (DA; 100 μ M). Traces represent the average of twenty replicates from five independent experiments. Signals were significantly smaller ($p=0.0036$) after activation of D2R; Welch's t-test. (B) BRET between the $G\beta\gamma$ sensor memGRKct-Nluc and Venus- $G\beta\gamma$ increases after activation of AT₁ or D2R. Traces represent the average of twenty replicates from five independent experiments. Signals were significantly larger ($p=0.0008$) after activation of D2R; Welch's t-test. Transfection was identical for panels A and B with the substitution of memGRKct-Nluc for HiBit-PLC β_3 -CAAX in panel B; G_{α_q} and $G_{\alpha_{i1}}$ were overexpressed together with Venus- $G\beta\gamma$ in both panels. (C) BRET between HiBit-PLC β_3 -CAAX wild-type (wt) and mutants with defective G_{α_q} binding to the distal CTD (EEE) or proximal CTD (LE). Traces represent the average of 32 replicates from eight independent experiments. Signals were significantly smaller for both mutants; one-way ANOVA with Dunnett's post-hoc comparisons.

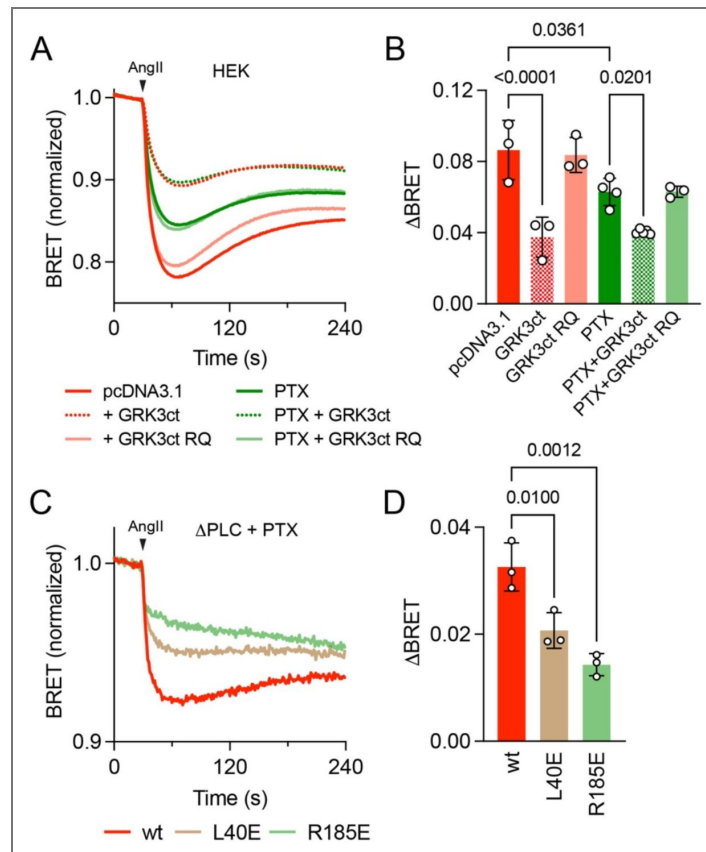


Figure S7. PLC β -mediated PIP₂ hydrolysis is facilitated by G β γ derived from both G_q and G_{i/o} heterotrimers.

(A) In HEK cells bystander BRET between Nluc-PH and mem-Venus decreases in response to AT₁ activation with AngII (1 μ M). Responses are inhibited by GRK3ct, which sequesters G β γ , but not the binding-defective R587Q mutant (GRKct RQ), both before and after inactivation of G_{i/o} heterotrimers with pertussis toxin (PTX). Traces are the average 12-16 replicates from 3-4 independent experiments. (B) Grouped data from the same experiments as panel A; indicated p values are from one-way ANOVA with Tukey's multiple comparisons test. (C) In Δ PLC cells expressing PTX, HiBit-PLC β 3 L40E and R185E mutants fail to fully reconstitute AngII-induced PIP₂ hydrolysis compared to the wild-type (wt) enzyme; traces are the average of twelve replicates from three independent experiments. (D) Grouped data from the same experiments as panel C; indicated p values are from one-way ANOVA with Dunnett's multiple comparisons test.

Table S1. Expression of HiBit-PLC β 3 variants as indicated by total LgBit-complemented luminescence in intact cells.

construct	raw luminescence (photons)			n
	mean	S.D.	P value [†]	
HiBit-PLC β 3	1.22E+07	6.27E+06	-	10
R24A	1.61E+07	6.51E+06	0.9768	3
R24E	3.25E+06	6.33E+05	0.1537	3
L40E	3.59E+06	1.26E+06	0.1905	3
L40K	2.62E+06	5.09E+05	0.1017	3
D167A	1.56E+07	4.73E+06	0.9928	3
D167G	1.27E+07	3.30E+06	>0.9999	3
R204A	1.85E+07	4.91E+06	0.6269	3
R204E	3.27E+06	5.89E+05	0.156	3
R24E+R204E	3.51E+06	1.30E+06	0.1809	3
R185E	1.23E+07	8.58E+06	>0.9999	4
R215A	1.19E+07	7.40E+06	>0.9999	3
R215E	1.21E+07	4.90E+06	>0.9999	3
L222K	1.37E+07	5.25E+06	>0.9999	4
F285E	8.39E+06	4.37E+06	0.9484	4
K183E	1.67E+07	6.30E+06	0.8662	4

[†]One-way ANOVA, Dunnett's multiple comparisons test vs. wild-type.

Table S2. Expression of HiBit-PLC β 3-CAAX variants as indicated by total LgBit-complemented luminescence in intact cells.

construct	raw luminescence (photons)			n
	mean	S.D.	P value [†]	
HiBit-PLC β 3-CAAX	1.54E+08	1.67E+08	-	7
R24A	2.51E+07	1.32E+07	0.1474	4
R24E	3.49E+07	2.05E+07	0.2216	4
L40E	3.65E+07	2.28E+07	0.2356	4
L40K	2.61E+07	1.37E+07	0.1539	4
D167A	2.75E+07	1.48E+07	0.1632	4
D167G	3.03E+07	1.94E+07	0.1833	4
R204A	3.76E+07	2.40E+07	0.2456	4
R204E	4.46E+07	2.76E+07	0.319	4
R24E+R204E	2.98E+07	1.54E+07	0.1797	4
R185E	2.43E+08	1.59E+08	0.719	3
R215A	3.15E+07	2.04E+07	0.1925	4
R215E	3.48E+07	2.49E+07	0.2203	4
L222K	1.91E+08	1.29E+08	0.9998	3
F285E	2.00E+08	1.11E+08	0.9976	3
K183E	1.55E+08	8.66E+07	>0.9999	3

[†]One-way ANOVA, Dunnett's multiple comparisons test vs. wild-type-CAAX.

Table S3. Angiotensin II-induced BRET between HiBit-PLC β 3-CAAX variants and Venus-G β y.

construct	Δ BRET			n
	mean	S.D.	P value [†]	
HiBit-PLC β 3-CAAX	0.01343	0.003746	-	10
+GRK3ct	-0.000968	0.001502	<0.0001	8
R24A	0.008984	0.001371	0.3104	5
R24E	0.004995	0.00116	0.0002	7
L40E	0.001863	0.00054	<0.0001	5
L40K	0.002092	0.00071	<0.0001	5
D167A	0.0306	0.01035	<0.0001	5
D167G	0.01943	0.004322	0.0517	5
R204A	0.007136	0.001778	0.0350	5
R204E	0.003198	0.000906	<0.0001	7
R24E+R204E	0.002536	0.001165	<0.0001	4
R185E	0.000937	0.000516	<0.0001	3
R215A	0.02478	0.00525	<0.0001	5
R215E	0.02706	0.006269	<0.0001	5
L222K	0.006882	0.00098	0.1052	3
F285E	0.002372	0.000248	0.0003	3
K183E	0.0116	0.002322	0.9984	4

[†]One-way ANOVA, Dunnett's multiple comparisons test vs. wild-type-CAAX.

Table S4. Angiotensin II-induced PIP2 hydrolysis mediated by HiBit-PLC β 3 variants.

construct	Δ BRET			n
	mean	S.D.	P value [†]	
HiBit-PLC β 3	0.05223	0.005327	-	11
+GRK3ct	0.02145	0.003139	<0.0001	11
R24A	0.053	0.008833	>0.9999	3
R24E	0.04107	0.004471	0.0030	5
L40E	0.02582	0.004777	<0.0001	5
L40K	0.02727	0.003389	<0.0001	5
D167A	0.07282	0.001987	<0.0001	3
D167G	0.06207	0.01019	0.0707	3
R204A	0.04634	0.002524	0.6770	3
R204E	0.03782	0.007242	<0.0001	5
R24E+R204E	0.03578	0.0041	<0.0001	4
R185E	0.01643	0.001868	<0.0001	3
R215A	0.06183	0.005277	0.0843	3
R215E	0.06154	0.006815	0.1041	3
L222K	0.02474	0.001306	<0.0001	3
F285E	0.01552	0.00182	<0.0001	3
K183E	0.03727	0.009687	0.0007	3

[†]One-way ANOVA, Dunnett's multiple comparisons test vs. wild-type.

Table S5. Angiotensin II-induced BRET between HiBit-PLC β 3 variants and G α q-Venus.

construct	Δ BRET			n
	mean	S.D.	P value [†]	
HiBit-PLC β 3	0.07705	0.01942	-	3
R24A	0.08169	0.01774	>0.9999	3
R24E	0.09379	0.01895	0.8153	3
L40E	0.105	0.01828	0.2442	3
L40K	0.07575	0.008115	>0.9999	3
D167A	0.1023	0.01475	0.3513	3
D167G	0.05385	0.01087	0.4539	3
R204A	0.0951	0.02177	0.7455	3
R204E	0.1066	0.01497	0.1925	3
R24E+R204E	0.1008	0.01792	0.4274	3
R185E	0.1094	0.02068	0.1247	3
R215A	0.1116	0.01287	0.0854	3
R215E	0.08856	0.01038	0.9817	3
L222K	0.08054	0.01358	>0.9999	3
F285E	0.05337	0.001885	0.4289	3
K183E	0.1021	0.007104	0.3642	3

[†]One-way ANOVA, Dunnett's multiple comparisons test vs. wild-type.

Table S6. Angiotensin II-induced BRET between HiBit-PLC β 3 variants and mem-Venus.

construct	Δ BRET			n
	mean	S.D.	P value [†]	
HiBit-PLC β 3	0.03366	0.003477	-	3
R24A	0.03012	0.00526	0.9390	3
R24E	0.03258	0.002824	>0.9999	3
L40E	0.03697	0.003716	0.9607	3
L40K	0.03456	0.002387	>0.9999	3
D167A	0.03445	0.003044	>0.9999	3
D167G	0.02822	0.003124	0.5771	3
R204A	0.03021	0.006573	0.9481	3
R204E	0.03401	0.004711	>0.9999	3
R24E+R204E	0.03131	0.003755	0.9978	3
R185E	0.02671	0.002865	0.2875	3
R215A	0.0381	0.004039	0.7947	3
R215E	0.03365	0.005771	>0.9999	3
L222K	0.03058	0.003968	0.9770	3
F285E	0.02902	0.002389	0.7545	3
K183E	0.02648	0.002579	0.2535	3

[†]One-way ANOVA, Dunnett's multiple comparisons test vs. wild-type.

Data availability

All assay data, including western blots, CPMB counts, and luminescence will be made available in the Purdue University Research Repository under a single DOI. Maps, half maps, and coordinate files were deposited in the PDB as 9Y7H, 9YAO, and 9YAP and in the EMDB as EMD-72655, EMD-72732, and EMD-72733.

Acknowledgements

We thank Steve Wilson and Drs. John. J. G. Tesmer, Val J. Watts, Thomas Klose, and Frank Vago for technical and conceptual assistance.

Additional information

Funding

A.I. was funded by Japan Society for the Promotion of Science (JP24K21281 and JP25H01016); Japan Science and Technology Agency (JPMJFR215T and JPMJMS2023); Japan Agency for Medical Research and Development (JP22ama121038 and JP22zf0127007); and The Uehara Memorial Foundation. E.K. was supported by the Deutsche Forschungsgemeinschaft (DFG, German Research Foundation) with the grant 214362475/GRK1873/3. This work is supported by F32GM145110-01 to I.J.F, R35GM145284 to N.A.L., 1R01HL141076 and 1R01GM152701 to A.M.L.

Funding

Funder	Grant reference number	Author
Japan Society for the Promotion of Science	JP24K21281	Asuka Inoue
MEXT Japan Society for the Promotion of Science (JSPS)	JP25H01016	Asuka Inoue
MEXT Japan Science and Technology Agency (JST)	https://doi.org/10.52926/jpmjfr215t	Asuka Inoue
MEXT Japan Science and Technology Agency (JST)	https://doi.org/10.52926/jpmjms2023	Asuka Inoue
Japan Agency for Medical Research and Development (AMED)	JP22ama121038	Asuka Inoue
Japan Agency for Medical Research and Development (AMED)	JP22zf0127007	Asuka Inoue
Uehara Memorial Foundation (UMF)		Asuka Inoue
Deutsche Forschungsgemeinschaft (DFG)	214362475/GRK1873/3	Evi Kostenis
HHS NIH National Heart, Lung, and Blood Institute (NHLBI)	1R01HL141076	Angeline Lyon
HHS NIH National Institute of General Medical Sciences (NIGMS)	F32GM145110-01	Isaac J Fisher
HHS NIH National Institute of General Medical Sciences (NIGMS)	R35GM145284	Nevin A Lambert
HHS NIH National Institute of General Medical Sciences (NIGMS)	1R01GM152701	Angeline Lyon

Author ORCID iDs

Eva Kostenis: <https://orcid.org/0000-0001-8284-5514>

Nevin A Lambert: <https://orcid.org/0000-0001-7550-0921>

Angeline M Lyon: <https://orcid.org/0000-0001-7501-0148>

References

1. Smrcka A. V., Sternweis P. C. (1993) Regulation of purified subtypes of phosphatidylinositol-specific phospholipase C β by G protein α and β subunits. *J Biol Chem* **268**:9667-9674 [https://doi.org/10.1016/s0021-9258\(18\)98401-2](https://doi.org/10.1016/s0021-9258(18)98401-2) | PubMed
2. Kadamur G., Ross E. M. (2013) Mammalian phospholipase C. *Annu Rev Physiol* **75**:127-154 <https://doi.org/10.1146/annurev-physiol-030212-183750> | PubMed
3. Lyon A. M., et al. (2011) An autoinhibitory helix in the C-terminal region of phospholipase C- β mediates G α_q activation. *Nat Struct Mol Biol* **18**:999-1005 <https://doi.org/10.1038/nsmb.2095> | PubMed
4. Waldo G. L., et al. (2010) Kinetic scaffolding mediated by a phospholipase C- β and G α_q signaling complex. *Science* **330**:974-980 <https://doi.org/10.1126/science.1193438> | PubMed
5. Lyon A. M., Dutta S., Boguth C. A., Skinnotis G., Tesmer J. J. (2013) Full-length Galpha(q)-phospholipase C-beta3 structure reveals interfaces of the C-terminal coiled-coil domain. *Nat Struct Mol Biol* **20**:355-362 <https://doi.org/10.1038/nsmb.2497> | PubMed
6. Senarath K., Fisher I. J., Jang W., Lu S., Inoue A., Kostenis E., Lyon A. M., Lambert N. A. (2025) An integrated mechanism of Gq regulation of PLC β enzymes. *Proceedings of the National Academy of Sciences* <https://doi.org/10.1073/pnas.2500318122> | PubMed
7. Smrcka A. V. (2008) G protein β subunits: central mediators of G protein-coupled receptor signaling. *Cell Mol Life Sci* **65**:2191-2214 <https://doi.org/10.1007/s00018-008-8006-5> | PubMed
8. Smrcka A. V., Fisher I. (2019) G-protein β subunits as multi-functional scaffolds and transducers in G-protein-coupled receptor signaling. *Cellular and Molecular Life Sciences* **76**:4447-4459 <https://doi.org/10.1007/s00018-019-03275-2> | PubMed
9. Jczyk M. R., et al. (2006) Crystal structure of Rac1 bound to its effector phospholipase C- β 2. *Nat Struct Mol Biol* **13**:1135-1140 <https://doi.org/10.1038/nsmb1175> | PubMed
10. Illenberger D., Walliser C., Nurnberg B., Diaz Lorente M., Gierschik P. (2003) Specificity and structural requirements of phospholipase C- β stimulation by Rho GTPases versus G protein β dimers. *J Biol Chem* **278**:3006-3014 <https://doi.org/10.1074/jbc.m208282200> | PubMed
11. Wang T., Dowal L., El-Maghrabi M. R., Rebecchi M., Scarlata S. (2000) The pleckstrin homology domain of phospholipase C- β 2 links the binding of G β to activation of the catalytic core. *J Biol Chem* **275**:7466-7469 <https://doi.org/10.1074/jbc.275.11.7466> | PubMed
12. Bonacci T. M., Ghosh M., Malik S., Smrcka A. V. (2005) Regulatory interactions between the amino terminus of G-protein β subunits and the catalytic domain of phospholipase C β 2. *J Biol Chem* **280**:10174-10181
13. Sankaran B., Osterhout J., Wu D., Smrcka A. V. (1998) Identification of a Structural Element in Phospholipase C β 2 That Interacts with G Protein β Subunits. *Journal of Biological Chemistry* **273**:7148-7154 <https://doi.org/10.1074/jbc.273.12.7148> | PubMed
14. Pfeil E. M., et al. (2020) Heterotrimeric G Protein Subunit G α_q Is a Master Switch for G $\beta\gamma$ -Mediated Calcium Mobilization by Gi-Coupled GPCRs. *Molecular Cell* **80**:940-954.e946 <https://doi.org/10.1016/j.molcel.2020.10.027> | PubMed
15. Brands J., et al. (2024) A molecular mechanism to diversify Ca $^{2+}$ signaling downstream of Gs protein-coupled receptors. *Nature Communications* **15** <https://doi.org/10.1038/s41467-024-51991-6> | PubMed
16. Gao Z.-G., Gao R. R., Meyer C. K., Jacobson K. A. (2025) A2B adenosine receptor-triggered intracellular calcium mobilization: Cell type-dependent involvement of Gi, Gq, Gs proteins and protein kinase C. *Purinergic Signalling* **21**:499-513 <https://doi.org/10.1007/s11302-025-10070-1> | PubMed

17. Falzone Maria E., MacKinnon R. (2023) G β activates PIP2 hydrolysis by recruiting and orienting PLC β on the membrane surface. *Proceedings of the National Academy of Sciences* **120** <https://doi.org/10.1073/pnas.2301121120> | PubMed
18. Romoser V., Ball R., Smrcka A. V. (1996) Phospholipase C β 2 association with phospholipid interfaces assessed by fluorescence resonance energy transfer. G protein β subunit-mediated translocation is not required for enzyme activation. *J Biol Chem* **271**:25071-25078
19. Runnels L. W., Jenco J., Morris A., Scarlata S. (1996) Membrane binding of phospholipases C-beta 1 and C-beta 2 is independent of phosphatidylinositol 4,5-bisphosphate and the alpha and beta gamma subunits of G proteins. *Biochemistry* **35**:16824-16832 <https://doi.org/10.1021/bi961606w> | PubMed
20. Runnels L. W., Scarlata S. F. (1998) Regulation of the Rate and Extent of Phospholipase C β 2 Effector Activation by the β Subunits of Heterotrimeric G Proteins. *Biochemistry* **37**:15563-15574 <https://doi.org/10.1021/bi9811258> | PubMed
21. Casey P. J. (1994) Lipid modifications of G proteins. *Current Opinion in Cell Biology* **6**:219-225 [https://doi.org/10.1016/0955-0674\(94\)90139-2](https://doi.org/10.1016/0955-0674(94)90139-2) | PubMed
22. Kadamur G., Ross E. M. (2016) Intrinsic Pleckstrin Homology (PH) Domain Motion in Phospholipase C-beta Exposes a Gbetagamma Protein Binding Site. *J Biol Chem* **291**:11394-11406 <https://doi.org/10.1074/jbc.m116.723940> | PubMed
23. Lee S., Shin S., Hepler J., Gilman A., Rhee S. (1993) Activation of phospholipase C- β 2 mutants by G protein α_q and β subunits. *J Biol Chem* **268**:25952-25957 [https://doi.org/10.1016/s0021-9258\(19\)74479-2](https://doi.org/10.1016/s0021-9258(19)74479-2) | PubMed
24. Banno Y., Asano T., Nozawa Y. (2001) Proteolytic modification of membrane-associated phospholipase C- β by μ -calpain enhances its activation by G-protein β subunits in human platelets. *FEBS Letters* **340**:185-188 [https://doi.org/10.1016/0014-5793\(94\)80134-7](https://doi.org/10.1016/0014-5793(94)80134-7) | PubMed
25. Fisher I. J., Jenkins M. L., Tall G. G., Burke J. E., Smrcka A. V. (2020) Activation of Phospholipase C β by G β and Gaq Involves C-Terminal Rearrangement to Release Autoinhibition. *Structure* **28**:810-819.e815 <https://doi.org/10.1016/j.str.2020.04.012> | PubMed
26. Lyon A. M., Tesmer J. J. (2013) Structural Insights into Phospholipase C-beta Function. *Mol Pharmacol* **84**:488-500 <https://doi.org/10.1124/mol.113.087403> | PubMed
27. Panchenko M. P., et al. (1998) Sites important for PLC β 2 activation by the G protein β subunit map to the sides of the beta propeller structure. *J Biol Chem* **273**:28298-28304 <https://doi.org/10.1074/jbc.273.43.28298> | PubMed
28. Drin G., Scarlata S. (2007) Stimulation of phospholipase C β by membrane interactions, interdomain movement, and G protein binding--how many ways can you activate an enzyme?. *Cell Signal* **19**:1383-1392 <https://doi.org/10.1016/j.cellsig.2007.04.006> | PubMed
29. Ford C. E., et al. (1998) Molecular basis for interactions of G protein β subunits with effectors. *Science* **280**:1271-1274 <https://doi.org/10.1126/science.280.5367.1271> | PubMed
30. Li Y., et al. (1998) Sites for G α binding on the G protein β subunit overlap with sites for regulation of phospholipase C β and adenylyl cyclase. *J Biol Chem* **273**:16265-16272 <https://doi.org/10.1074/jbc.273.26.16265> | PubMed
31. Atef M. E., Anand-Srivastava M. B. (2016) Oxidative stress contributes to the enhanced expression of Gqalpha/PLCbeta1 proteins and hypertrophy of VSMC from SHR: role of growth factor receptor transactivation. *Am J Physiol Heart Circ Physiol* **310**:H608-618 <https://doi.org/10.1152/ajpheart.00659.2015> | PubMed
32. Calizo R. C., et al. (2020) Cell shape regulates subcellular organelle location to control early Ca $^{2+}$ signal dynamics in vascular smooth muscle cells. *Scientific reports* **10** <https://doi.org/10.1038/s41598-020-74700-x> | PubMed

33. Filtz T. M., Grubb D. R., McLeod-Dryden T. J., Luo J., Woodcock E. A. (2009) G_q-initiated cardiomyocyte hypertrophy is mediated by phospholipase Cβ1b. *FASEB J* **23**:3564-3570 <https://doi.org/10.1096/fj.09-133983> | PubMed
34. Mathews J. L., Smrcka A. V., Bidlack J. M. (2008) A Novel G_i-Subunit Inhibitor Selectively Modulates - Opioid-Dependent Antinociception and Attenuates Acute Morphine-Induced Antinociceptive Tolerance and Dependence. *Journal of Neuroscience* **28**:12183-12189 <https://doi.org/10.1523/jneurosci.2326-08.2008> | PubMed
35. Xie W., et al. (1999) Genetic alteration of phospholipase C β3 expression modulates behavioral and cellular responses to μ opioids. *Proc Natl Acad Sci U S A* **96**:10385-10390 <https://doi.org/10.1073/pnas.96.18.10385> | PubMed
36. Waldo G. L., Paterson A., Boyer J. L., Nicholas R. A., Harden T. K. (1996) Molecular cloning, expression and regulatory activity of Gα₁₁- and βγ-subunit-stimulated phospholipase C-β from avian erythrocytes. *Biochem J* **316**:559-568 <https://doi.org/10.1042/bj3160559> | PubMed
37. Charpentier T. H., et al. (2014) Membrane-induced allosteric control of phospholipase C-beta isozymes. *J Biol Chem* **289**:29545-29557
38. Feng J., Roberts M. F., Drin G., Scarlata S. (2005) Dissection of the steps of phospholipase Cβ 2 activity that are enhanced by Gβγ subunits. *Biochemistry* **44**:2577-2584 <https://doi.org/10.1021/bi0482607> | PubMed
39. Han D. S., Golebiewska U., Stolzenberg S., Scarlata S. F., Weinstein H. (2011) A dynamic model of membrane-bound phospholipase Cβ2 activation by Gβγ subunits. *Mol Pharmacol* **80**:434-445 <https://doi.org/10.1124/mol.111.073403> | PubMed
40. Barr A. J., Ali H., Haribabu B., Snyderman R., Smrcka A. V. (2000) Identification of a region at the N-terminus of phospholipase C-β 3 that interacts with G protein βγ subunits. *Biochemistry* **39**:1800-1806 <https://doi.org/10.1021/bi992021f> | PubMed
41. Chen C.-L., et al. (2024) Molecular basis for Gβγ-mediated activation of phosphoinositide 3-kinase γ. *Nature Structural & Molecular Biology* **31**:1198-1207 <https://doi.org/10.1038/s41594-024-01265-y> | PubMed
42. Rathinaswamy M. K., et al. (2021) Structure of the phosphoinositide 3-kinase (PI3K) p110γ-p101 complex reveals molecular mechanism of GPCR activation. *Science Advances* **7** <https://doi.org/10.1126/sciadv.abj4282> | PubMed
43. Lee C. W., Lee K. H., Lee S. B., Park D., Rhee S. G. (1994) Regulation of phospholipase C-β 4 by ribonucleotides and the α subunit of G_q. *J Biol Chem* **269**:25335-25338 [https://doi.org/10.1016/s0021-9258\(18\)47252-3](https://doi.org/10.1016/s0021-9258(18)47252-3) | PubMed
44. Lee C. W., Park D. J., Lee K. H., Kim C. G., Rhee S. G. (1993) Purification, molecular cloning, and sequencing of phospholipase C-beta 4. *J Biol Chem* **268**:21318-21327 [https://doi.org/10.1016/s0021-9258\(19\)36926-1](https://doi.org/10.1016/s0021-9258(19)36926-1) | PubMed
45. Rebres R. A., et al. (2011) Synergistic Ca²⁺ responses by Gα_i- and Gα_q-coupled G-protein-coupled receptors require a single PLCβ isoform that is sensitive to both Gβγ and Gα_q. *J Biol Chem* **286**:942-951 <https://doi.org/10.1074/jbc.m110.198200> | PubMed
46. Sanchez G. A., Jutkiewicz E. M., Ingram S., Smrcka A. V. (2022) Coincident Regulation of PLCβ Signaling by Gq-Coupled and μ-Opioid Receptors Opposes Opioid-Mediated Antinociception. *Molecular Pharmacology* **102**:269-279 <https://doi.org/10.1124/molpharm.122.000541> | PubMed
47. Kankanamge D., et al. (2021) Dissociation of the G protein βγ from the Gq-PLCβ complex partially attenuates PIP2 hydrolysis. *Journal of Biological Chemistry* **296** <https://doi.org/10.1016/j.jbc.2021.100702> | PubMed
48. de Rubio R. G., et al. (2018) Phosphatidylinositol 4-phosphate is a major source of GPCR-stimulated phosphoinositide production. *Science Signaling* **11** <https://doi.org/10.1126/scisignal.aan1210> | PubMed

49. Davis T. L., Bonacci T. M., Sprang S. R., Smrcka A. V. (2005) Structural and molecular characterization of a preferred protein interaction surface on G protein $\beta\gamma$ subunits. *Biochemistry* **44**:10593-10604 <https://doi.org/10.1021/bi050655i> | PubMed
50. Kozasa T. (1999) Purification of recombinant G protein α and $\beta\gamma$ subunits from Sf9 cells. In: Manning D. R. (Ed). *G Proteins : Techniques of Analysis* CRC Press LLC. pp. 23-37
51. Ghosh M., Smrcka A. V. (2004) Assay for G protein-dependent activation of phospholipase C β using purified protein components. *Methods Mol Biol* **237**:67-75
52. Ghosh M., Wang H., Kelley G. G., Smrcka A. V. (2004) Purification of phospholipase C β and phospholipase C ϵ from Sf9 cells. *Methods Mol Biol* **237**:55-64
53. Punjani A., Rubinstein J. L., Fleet D. J., Brubaker M. A. (2017) cryoSPARC: algorithms for rapid unsupervised cryo-EM structure determination. *Nature Methods* **14**:290-296 <https://doi.org/10.1038/nmeth.4169> | PubMed
54. Trabuco L. G., Villa E., Schreiner E., Harrison C. B., Schulten K. (2009) Molecular dynamics flexible fitting: A practical guide to combine cryo-electron microscopy and X-ray crystallography. *Methods* **49**:174-180 <https://doi.org/10.1016/j.ymeth.2009.04.005> | PubMed
55. Casañal A., Lohkamp B., Emsley P. (2020) Current developments in Coot for macromolecular model building of Electron Cryo-microscopy and Crystallographic Data. *Protein Science* **29**:1055-1064 <https://doi.org/10.1002/pro.3791> | PubMed
56. Adams P. D., et al. (2010) PHENIX: a comprehensive Python-based system for macromolecular structure solution. *Acta Crystallogr D Biol Crystallogr* **66**:213-221 <https://doi.org/10.1107/s0907444909052925> | PubMed
57. Liebschner D., et al. (2019) Macromolecular structure determination using X-rays, neutrons and electrons: recent developments in Phenix. *Acta Crystallographica Section D Structural Biology* **75**:861-877 <https://doi.org/10.1107/s2059798319011471> | PubMed
58. Jang W., Senarath K., Feinberg G., Lu S., Lambert N. A. (2024) Visualization of endogenous G proteins on endosomes and other organelles. *eLife* **13** <https://doi.org/10.7554/elife.97033> | PubMed
59. Madukwe J. C., Garland-Kuntz E. E., Lyon A. M., Smrcka A. V. (2018) G protein betagamma subunits directly interact with and activate phospholipase Cepsilon. *J Biol Chem* <https://doi.org/10.1074/jbc.RA118.002354> | PubMed
60. Kozasa T., Gilman A. (1995) Purification of recombinant G proteins from Sf9 cells by hexahistidine tagging of associated subunits. Characterization of α_{12} and inhibition of adenylyl cyclase by az. *J Biol Chem* **270**:1734-1741
61. Zheng S. Q., et al. (2017) MotionCor2: anisotropic correction of beam-induced motion for improved cryo-electron microscopy. *Nature Methods* **14**:331-332 <https://doi.org/10.1038/nmeth.4193> | PubMed
62. Rohou A., Grigorieff N. (2015) CTFIND4: Fast and accurate defocus estimation from electron micrographs. *Journal of Structural Biology* **192**:216-221 <https://doi.org/10.1016/j.jsb.2015.08.008> | PubMed
63. Wall M. A., et al. (1995) The structure of the G protein heterotrimer $G_{i1}\alpha_1\beta_1\gamma_2$. *Cell* **83**:1047-1058 [https://doi.org/10.1016/0092-8674\(95\)90220-1](https://doi.org/10.1016/0092-8674(95)90220-1) | PubMed
64. Pettersen E. F., et al. (2004) UCSF Chimera—A visualization system for exploratory research and analysis. *J Comput Chem* **25**:1605-1612 <https://doi.org/10.1002/jcc.20084> | PubMed
65. Terashi G., Wang X., Kihara D. (2023) Protein model refinement for cryo-EM maps using AlphaFold2 and the DAQ score. *Acta Crystallographica Section D Structural Biology* **79**:10-21 <https://doi.org/10.1107/s2059798322011676> | PubMed
66. Terashi G., Wang X., Maddhuri Venkata Subramaniya S. R., Tesmer J. J. G., Kihara D. (2022) Residue-wise local quality estimation for protein models from cryo-EM maps. *Nature Methods* **19**:1116-1125 <https://doi.org/10.1038/s41592-022-01574-4> | PubMed

Peer reviews

Reviewer #1 (Public review):

The manuscript by Fisher et al describes the molecular mechanism underlying how G beta gamma subunits engage with the beta 3 isoform of PLC. The paper used a combination of cryo EM, BRET assays, and biochemical assays of PLC beta activity. A key discovery is that G beta gamma is not sufficient to drive membrane binding by itself, and instead promotes G alpha activation. The work is important, but suffers slightly from some ambiguity in the actual interface that is present in their cryo EM model, as crosslinkers could stabilise a transient and non-native complex. This is somewhat abrogated by the careful mutational analysis, which shows that mutation of any of these three sites does somewhat block PLC beta G beta gamma activation. However, there could be some improvement in the presentation of this data, as well as possible mutant selection. Overall, this paper is a nice complement to the Falzone et al paper, showing the membrane-bound complex of PLCB3 on membranes, with this work building on this work, highlighting the importance this will have in our full understanding of PLC beta activation.

Major concerns:

My biggest concern is the potential that this interface is artefactual based on the crosslinking strategy utilised. Here are thoughts on how this could be better validated, presented in a more convincing way.

(1) The authors' main claim is that there is a degree of plasticity of G beta gamma binding to the PLC beta 3 isoform, with three possible binding sites. The main complication of this is, of course, the possibility that the crosslinking stabilises a non-native complex, driven by a mutated cysteine.

Because of this, any other additional details about this interface are going to be critical for the scientific audience to judge if this is accurate.

What would greatly help Figure 1 is an evolutionary conservation analysis of the novel Gbg interface in PLC, to see how well this is conserved, and compare this to the conservation of the previously annotated sites. Conservation of these sites on both the G beta gamma and PLC side would help justify this as a native complex.

This will also help orient the reader to the identity of the mutated residues assayed in Figure 3.

(2) The g beta gamma orientation is also different than what I have observed in previous g beta gamma effector structures. Is there any precedent for this as an effector interface? A supplemental figure comparing this structure to other g beta gamma interfaces from other enzymes, for example recent Tesmer structure with PI3K.

(3) The mutational analysis in Figure 2D-G seems to give some strange results, and I have some question why certain residues were chosen rather than others. Mutation of the Gbg side will be more complicated, as of course that can affect any of the three surfaces. My main question is that, from the way Figure 2A is oriented, the main salt bridge in their novel interface to me looks like R199-D228, with K183 being in the wrong orientation to E226, and D167 being far from any charged residues. Why did the authors not make the corresponding R199 to D or E mutation?

(4) To help the reader's interpretation of Figure 2A, I would recommend a supplemental figure showing the density for interfacial residues, as that also would increase confidence in the interface.

<https://doi.org/10.7554/eLife.110382.1.sa3>

Reviewer #2 (Public review):

In this manuscript, the authors dissect how G $\beta\gamma$ potentiates PLC β 3 signaling in cells. Using engineered crosslinking to stabilize a G $\beta\gamma$ -PLC β 3 complex, single particle cryo-EM, and cell-based functional assays, they identify and map multiple putative G $\beta\gamma$ interaction surfaces on PLC β 3, including a previously unrecognized binding mode. Structure-guided mutagenesis supports the functional relevance of these interactions and suggests that G $\beta\gamma$ potentiation is not primarily mediated by PLC β 3 membrane recruitment, but instead enhances PLC β 3 activity after the lipase is already at the membrane.

Previous reconstitution work on the membrane surface (Falzone & MacKinnon, 2023) proposed a recruitment/partitioning-centric model in which G $\beta\gamma$ increases PLC β 3 output largely by elevating its membrane surface concentration, whereas G α_q primarily increases catalytic turnover; under those reconstitution conditions, the two inputs can combine approximately multiplicatively. In receptor-driven cellular signaling, however, PLC β 3 is robustly recruited to the plasma membrane upon G α_q activation, which raises the question of whether G $\beta\gamma$ contributes mainly through additional recruitment or through a post-recruitment mechanism once PLC β 3 is already at the membrane.

This manuscript helps address that gap by using membrane-anchored PLC β 3 and complementary cellular readouts to separate "getting PLC β 3 to the membrane" from "boosting activity once PLC β 3 is already there." Their results argue that, in cells, membrane recruitment is largely dominated by G α_q -GTP, while G $\beta\gamma$ can further potentiate PIP2 hydrolysis after membrane association, consistent with a modulatory role at the membrane rather than primary recruitment.

Overall, the work provides a structural and mechanistic framework for G $\beta\gamma$ -PLC β 3 cooperation and helps clarify the basis of G α_q pathway amplification. The manuscript is generally strong, but some issues need to be addressed.

Major comments:

(1) BMOE/BM(PEG)2 crosslinking may enforce a non-native docking geometry, potentially compromising the physiological relevance and precision of the G $\beta\gamma$ -PLC β 3 interface as described. Although a >50% 1:1 crosslinked complex is formed and remains active, the solution maps show lower local resolution for G $\beta\gamma$, consistent with a dynamic, potentially heterogeneous, interface. One interface is captured via a single engineered cysteine pair (PLC β 3 E60C-G β C271), which could potentially bias the pose. It would be helpful if the authors could provide additional orthogonal support (e.g., alternative crosslinked sites) and bolster the clarification of its uniqueness and relevance.

(2) In the crosslinked structure, the authors report that G β D228 interacts with PLC β 3 R199 and K183. In Figure 2A, R199 appears closer to G β D228 than K183, yet only K183 is functionally tested. Testing R199 (e.g., R199E/R199A) would strengthen the structure-guided validation of this interface.

(3) The mutagenesis strategy appears inconsistent across figures/assays, which makes it difficult to interpret phenotypes and directly link the functional data to the proposed interfaces. For example, in Figure 2E, we see R185L but R215E, while residue L40 is mutated to Gly in the IP accumulation assays but to Glu/Lys (L40E/K) in the BRET assays (Figures 3B/3D/3F). The authors should (i) clearly justify the rationale for each substitution (conservative vs charge-reversal, interface disruption, etc.) and (ii), where possible, test the same mutants across assays (or provide evidence that alternative substitutions yield consistent conclusions).

<https://doi.org/10.7554/eLife.110382.1.sa2>

Reviewer #3 (Public review):

Summary:

PLC β 3 is activated by both G α q and G $\beta\gamma$ subunits. This paper follows previous solutions and cryoEM studies of PLC β 3 / G $\beta\gamma$, trying to understand the molecular details of activation using cellular BRET assays and cryoEM.

Strengths:

The authors find evidence for multiple binding sites on PLC β 3 for G $\beta\gamma$ and suggest that G $\beta\gamma$ is not bone fide activator per se but enhances G α q activation by positioning the catalytic site towards substrate, although this is not completely convincing. Although these sites may not naturally be operative, the authors might want to develop the potential role of these sites.

The authors also find that this activation is not through recruitment of the enzyme to the membrane by G $\beta\gamma$ released upon G protein activation, in accord with other PLC β enzymes, but not for PLC β 3, and again, the authors might want to develop this point further.

Weaknesses:

(1) I'm confused as to why the authors feel that their mechanism is distinct from the two-state enzyme, the synergistic activation proposed by Ross in 2011, using a primarily thermodynamic argument. As written, the authors appear to be very reliant on structural and BRET studies that do not give the details that would disprove this interpretation. The main issue is that the author's mechanism does not fully explain how G $\beta\gamma$ activation occurs for PLC β 2 in reconstituted systems in the absence of G α q subunits.

(2) In a recent study, McKinnon presents a model showing that G α q and G $\beta\gamma$ activate PLC β 3 by two distinct pathways and that activation by G $\beta\gamma$ occurs through membrane recruitment. It is not surprising that the authors find that this is not true since the pelleting method used by McKinnon is subject to error. The authors should directly address the limitations of this previous work and the changes in proteoliposomes with sedimentation that alter partition coefficients. Although the inability of G $\beta\gamma$ to drive membrane binding is in accord with the quantitative studies of Scarlata, showing that the affinity of PLC β 3 to G $\beta\gamma$ is fairly weak as compared to the intrinsic membrane partition coefficient.

(3) It was proposed many years ago that in signaling complexes G α q - G $\beta\gamma$ may not have to fully dissociate when binding PLC β , but rather shift their relative orientation when binding to PLC β to allow activation. Is their model consistent with this? Is it possible that PLC β 3 keeps G $\beta\gamma$ from diffusing to enhance the rate of G α q / G $\beta\gamma$ re-association?

(4) The authors find that G $\beta\gamma$ binds multiple sites, and it is clear that the PH domain site is the primary one in accord with previous work. Could these weaker sites be an artifact of the elevated concentrations used in cryoEM and BRET assays?

(5) Although their assays infer differences in binding affinities, it would strengthen the paper if the authors could estimate the association energies of these different binding sites. This estimation would also address the concern stated above.

<https://doi.org/10.7554/eLife.110382.1.sa1>

Author Response:

Public Reviews:**Reviewer #1 (Public review):**

The manuscript by Fisher et al describes the molecular mechanism underlying how G beta gamma subunits engage with the beta 3 isoform of PLC. The paper used a combination of cryo EM, BRET assays, and biochemical assays of PLC beta activity. A key discovery is that G beta gamma is not sufficient to drive membrane binding by itself, and instead promotes G alpha activation. The work is important, but suffers slightly from some ambiguity in the actual interface that is present in their cryo EM model, as crosslinkers could stabilise a transient and non-native complex. This is somewhat abrogated by the careful mutational analysis, which shows that mutation of any of these three sites does somewhat block PLC beta G beta gamma activation. However, there could be some improvement in the presentation of this data, as well as possible mutant selection. Overall, this paper is a nice complement to the Falzone et al paper, showing the membrane-bound complex of PLCB3 on membranes, with this work building on this work, highlighting the importance this will have in our full understanding of PLC beta activation.

Thank you for the positive feedback.

Major concerns:

My biggest concern is the potential that this interface is artefactual based on the crosslinking strategy utilised. Here are thoughts on how this could be better validated, presented in a more convincing way.

(1) The authors' main claim is that there is a degree of plasticity of G beta gamma binding to the PLC beta 3 isoform, with three possible binding sites. The main complication of this is, of course, the possibility that the crosslinking stabilises a non-native complex, driven by a mutated cysteine.

Because of this, any other additional details about this interface are going to be critical for the scientific audience to judge if this is accurate.

What would greatly help Figure 1 is an evolutionary conservation analysis of the novel Gbg interface in PLC, to see how well this is conserved, and compare this to the conservation of the previously annotated sites. Conservation of these sites on both the G beta gamma and PLC side would help justify this as a native complex.

This will also help orient the reader to the identity of the mutated residues assayed in Figure 3.

We agree that crosslinking can result in the capture a non-physiologically relevant interface. However, we do not observe any crosslinking between Gbg and a PLCb3 variant that retains a cysteine in the disordered region of the X–Y linker, nor crosslinking between PLCb3 and any other cysteine present in the Gbg heterodimer. The evolutionary conservation analysis is a great suggestion and will included in the revision for both Gbg and PLCb.

(2) The g beta gamma orientation is also different than what I have observed in previous g beta gamma effector structures. Is there any precedent for this as an effector interface? A supplemental figure comparing this structure to other g beta gamma interfaces from other enzymes, for example recent Tesmer structure with PI3K.

Yes, this is not the more typically observed Gbg–effector interaction, which is mediated by the narrow face of the Gbg-toroid. We are not aware of other structures in which Gbg interacts

with a binding partner in the same way. A supplemental figure comparing this Gbg-PLCb interaction to the Gbg-PI3K and Gbg-GRK2 structures will be included in the revision.

(3) *The mutational analysis in Figure 2D-G seems to give some strange results, and I have some question why certain residues were chosen rather than others. Mutation of the Gbg side will be more complicated, as of course that can affect any of the three surfaces. My main question is that, from the way Figure 2A is oriented, the main salt bridge in their novel interface to me looks like R199-D228, with K183 being in the wrong orientation to E226, and D167 being far from any charged residues. Why did the authors not make the corresponding R199 to D or E mutation?*

Thank you for pointing this out. We are in the process of testing the PLCb3 R199E mutant in our assays and will include the results in the revised manuscript.

(4) *To help the reader's interpretation of Figure 2A, I would recommend a supplemental figure showing the density for interfacial residues, as that also would increase confidence in the interface.*

Thank you for the suggestion, this will be included in the revised manuscript.

Reviewer #2 (Public review):

In this manuscript, the authors dissect how Gβγ potentiates PLCβ3 signaling in cells. Using engineered crosslinking to stabilize a Gβγ-PLCβ3 complex, single particle cryo-EM, and cell-based functional assays, they identify and map multiple putative Gβγ interaction surfaces on PLCβ3, including a previously unrecognized binding mode. Structure-guided mutagenesis supports the functional relevance of these interactions and suggests that Gβγ potentiation is not primarily mediated by PLCβ3 membrane recruitment, but instead enhances PLCβ3 activity after the lipase is already at the membrane.

Previous reconstitution work on the membrane surface (Falzone & MacKinnon, 2023) proposed a recruitment/partitioning-centric model in which Gβγ increases PLCβ3 output largely by elevating its membrane surface concentration, whereas Gαq primarily increases catalytic turnover; under those reconstitution conditions, the two inputs can combine approximately multiplicatively. In receptor-driven cellular signaling, however, PLCβ3 is robustly recruited to the plasma membrane upon Gαq activation, which raises the question of whether Gβγ contributes mainly through additional recruitment or through a post-recruitment mechanism once PLCβ3 is already at the membrane.

This manuscript helps address that gap by using membrane-anchored PLCβ3 and complementary cellular readouts to separate "getting PLCβ3 to the membrane" from "boosting activity once PLCβ3 is already there." Their results argue that, in cells, membrane recruitment is largely dominated by Gαq-GTP, while Gβγ can further potentiate PIP2 hydrolysis after membrane association, consistent with a modulatory role at the membrane rather than primary recruitment.

Overall, the work provides a structural and mechanistic framework for Gβγ-PLCβ3 cooperation and helps clarify the basis of Gq pathway amplification. The manuscript is generally strong, but some issues need to be addressed.

Thank you for the positive comments.

Major comments:

(1) *BMOE/BM(PEG)2 crosslinking may enforce a non-native docking geometry, potentially compromising the physiological relevance and precision of the Gβγ-PLCβ3 interface as described. Although a >50% 1:1 crosslinked complex is formed and remains active, the solution maps show lower local resolution for Gβγ, consistent with a dynamic, potentially*

heterogeneous, interface. One interface is captured via a single engineered cysteine pair (PLCβ3 E60C-Gβ C271), which could potentially bias the pose. It would be helpful if the authors could provide additional orthogonal support (e.g., alternative crosslinked sites) and bolster the clarification of its uniqueness and relevance.

We did attempt to isolate other crosslinked complexes. PLCb3-D892 self-crosslinked under all reaction conditions, while PLCb3-D892 XY_{Cys}, which retains an endogenous cysteine within the X-Y linker (C516), did not result in any crosslinked product when incubated with Gbg. Only the PLCb3-D892 E60C crosslinked to Gbg as confirmed by SDS-PAGE and SEC. All experiments also used wild-type Gb which contains two solvent-exposed cysteines in the effector binding site (C204 and C271). The greatest number of particles correspond to crosslinking between Gb C271 and E60C in PLCb3-D892. Crosslinking between PLCb3-D892 E60C and other residues in Gbg is possible, but there are not sufficient particle numbers corresponding to these species for 2D classing and reconstruction. These observations, together with the high efficiency of crosslinking, are consistent with a stable and persistent interaction.

(2) In the crosslinked structure, the authors report that GβD228 interacts with PLCβ3 R199 and K183. In Figure 2A, R199 appears closer to Gβ D228 than K183, yet only K183 is functionally tested. Testing R199 (e.g., R199E/R199A) would strengthen the structure-guided validation of this interface.

We agree, and functional analysis of PLCb3 R199E will be included in the revision.

(3) The mutagenesis strategy appears inconsistent across figures/assays, which makes it difficult to interpret phenotypes and directly link the functional data to the proposed interfaces. For example, in Figure 2E, we see R185L but R215E, while residue L40 is mutated to Gly in the IP accumulation assays but to Glu/Lys (L40E/K) in the BRET assays (Figures 3B/3D/3F). The authors should (i) clearly justify the rationale for each substitution (conservative vs charge-reversal, interface disruption, etc.) and (ii), where possible, test the same mutants across assays (or provide evidence that alternative substitutions yield consistent conclusions).

The mutagenesis experiments were initially carried out independently in the Lambert and Lyon groups. As the study progressed, additional mutations were designed based on prior results. The L40G mutation is one such example. Given its modest impact on activity in the IP accumulation assay, the L40E and L40K mutants designed to maximally disrupt the interface in the BRET experiments. The revision will include the rationale behind different substitutions and discussion of any potential differences.

Reviewer #3 (Public review):

Summary:

PLCβ3 is activated by both Gaq and Gβγ subunits. This paper follows previous solutions and cryoEM studies of PLCβ3 / Gβγ, trying to understand the molecular details of activation using cellular BRET assays and cryoEM.

Strengths:

The authors find evidence for multiple binding sites on PLCβ3 for Gβγ and suggest that Gβγ is not bone fide activator per se but enhances Gaq activation by positioning the catalytic site towards substrate, although this is not completely convincing. Although these sites may not naturally be operative, the authors might want to develop the potential role of these sites.

The authors also find that this activation is not through recruitment of the enzyme to the membrane by Gβγ released upon G protein activation, in accord with other PLCβ enzymes, but not for PLCβ3, and again, the authors might want to develop this point further.

Thank you for the suggestions.

Weaknesses:

(1) I'm confused as to why the authors feel that their mechanism is distinct from the two-state enzyme, the synergistic activation proposed by Ross in 2011, using a primarily thermodynamic argument. As written, the authors appear to be very reliant on structural and BRET studies that do not give the details that would disprove this interpretation. The main issue is that the author's mechanism does not fully explain how Gβγ activation occurs for PLCβ2 in reconstituted systems in the absence of Gαq subunits.

The reconstitution experiments rely on nM-mM concentrations of purified proteins and liposomes that contain up to 30% PI (4,5)P₂. PLCβ2 and PLCβ3 show dose-dependent increases in activity with increasing concentrations of Gβγ. PLCβ enzymes that interact with the liposomes would encounter liposome-tethered Gβγ subunits, which would in turn bind the lipase, tethering to the membrane and helping position the active site for catalysis. While there is not yet experimental evidence that Gβγ binding can displace the Ha2' helix, it could facilitate interfacial activation given the net negative charge of PI (4,5)P₂. In addition, PLCβ2 is fundamentally different from the other PLCβ isoforms in its sensitivity to heterotrimeric G proteins. Given its decreased sensitivity to Gα_q and increased basal activity, it is possible that autoinhibition by the proximal CTD is weaker. PLCβ2 is also abundantly expressed in neutrophils, along with more Gi-coupled receptors. Thus, it is possible that Gβγ directly activates PLCβ2 in these cells, but future experiments are required to definitively answer this question.

(2) In a recent study, McKinnon presents a model showing that Gαq and Gβγ activate PLCβ3 by two distinct pathways and that activation by Gβγ occurs through membrane recruitment. It is not surprising that the authors find that this is not true since the pelleting method used by McKinnon is subject to error. The authors should directly address the limitations of this previous work and the changes in proteoliposomes with sedimentation that alter partition coefficients. Although the inability of Gβγ to drive membrane binding is in accord with the quantitative studies of Scarlata, showing that the affinity of PLCβ3 to Gβγ is fairly weak as compared to the intrinsic membrane partition coefficient.

Thank you for raising this point. The changes in composition, size, and structure when pelleting proteoliposomes may complicate data interpretation and will be discussed in the revision.

(3) It was proposed many years ago that in signaling complexes Gαq - Gβγ may not have to fully dissociate when binding PLCβ, but rather shift their relative orientation when binding to PLCβ to allow activation. Is their model consistent with this? Is it possible that PLCβ3 keeps Gβγ from diffusing to enhance the rate of Gαq / Gβγ re-association?

The crosslinked complex is compatible with simultaneous binding of a Gβγ-Gβγ heterotrimer to the PLCβ3 without disrupting the observed interface. It is possible that Gβγ could interact with Gβγ bound to the PH domain or the EF hands in the previously reported reconstruction. If so, the interaction would be mediated by the N-terminal helix of Gβγ. Alternatively, the intrinsic GAP activity of PLCβ3 may also prevent Gβγ from diffusing to promote heterotrimer reassociation.

(4) The authors find that G β binds multiple sites, and it is clear that the PH domain site is the primary one in accord with previous work. Could these weaker sites be an artifact of the elevated concentrations used in cryoEM and BRET assays?

Assuming the PH domain is the primary G β binding site, it is possible that the secondary EF hand site observed by Falzone and Mackinnon reflects high protein concentrations. However, it seems unlikely that we would reach these concentrations within cells. Our functional data is also consistent with the G β binding site in the EF hands playing a functional role in increasing PLC β activity.

(5) Although their assays infer differences in binding affinities, it would strengthen the paper if the authors could estimate the association energies of these different binding sites. This estimation would also address the concern stated above.

We appreciate this suggestion and will keep it in mind as we complete the revision.

<https://doi.org/10.7554/eLife.110382.1.sa0>